

Simultaneous Perturbation Methods for Adaptive Labor Staffing in Service Systems

Prashanth L.A.[†], H.L. Prasad[#], Nirmal Desai[§], Shalabh Bhatnagar[#] and Gargi Dasgupta[§]

[†]Sequel Team, INRIA Lille - Nord Europe, FRANCE

[#]Department of Computer Science and Automation, Indian Institute of Science, INDIA

[§]IBM Research, INDIA

Abstract

Service systems are labor intensive due to the large variation in the tasks required to address service requests from multiple customers. Aligning the staffing levels to the forecasted workloads adaptively in such systems is nontrivial because of a large number of parameters and operational variations leading to a huge search space. A challenging problem here is to optimize the staffing while maintaining the system in steady-state and compliant to aggregate service level agreement (SLA) constraints. Further, because these parameters change on a weekly basis, the optimization should not take longer than a few hours. We formulate this problem as a constrained Markov cost process parameterized by the (discrete) staffing levels. We propose novel simultaneous perturbation stochastic approximation (SPSA) based SASOC (Staff Allocation using Stochastic Optimization with Constraints) algorithms for solving the above problem. The algorithms include both first order as well as second order methods and incorporate SPSA based gradient estimates in the primal, with dual ascent for the Lagrange multipliers. Both the algorithms that we propose are online, incremental and easy to implement. Further, they involve a certain generalized smooth projection operator, which is essential to project the continuous-valued worker parameter tuned by SASOC algorithms onto the discrete set. We validated our algorithms on five real-life service systems and compared them with a state-of-the-art optimization tool-kit OptQuest. Being 25 times faster than OptQuest, our algorithms are particularly suitable for adaptive labor staffing. Also, we observe that our algorithms guarantee convergence and find better solutions than OptQuest in many cases.

Keywords: Service systems, labor optimization, Adaptive labor staffing, Simultaneous perturbation stochastic approximation.

1 Introduction

A *Service System (SS)* is an organization composed of (i) the resources that support, and (ii) the processes that drive service interactions so that the outcomes meet customer expectations ((Alter 2008; Spohrer et al. 2007)). This paper focuses on SS in the data-center management domain, where customers own data centers and other IT infrastructures supporting their businesses. Owing to size, complexity, and uniqueness of these technology installations, the management responsibilities of the same are outsourced to specialized service providers. A *delivery center* is a remotely located workplace from where the service providers manage the data-centers. Each *service request (SR)* that arrives at a delivery center requires a specific skill and is supported by a *service worker (SW)* with the corresponding skill set. The SWs work in shifts which are typically aligned to the business hours of the supported customers. Hence, a group of customers supported by a group of SWs, along with the operational model of how SRs are routed constitutes an SS in this paper. A delivery center may consist of many SS.

We consider the problem of adaptive labor staffing in the context of service systems. The objective is to find the optimal staffing levels in a SS for a given dispatching policy (i.e., a map from service requests to service workers) while maintaining system steady-state and compliance to aggregate service level agreement (SLA) constraints. The staffing levels constitute the worker parameter that we optimize and specify the number of workers in each shift and of each skill level. The SLA constraints specify the target resolution time and the aggregate percentage for an SR originating from a particular customer and with a specified priority level. For instance, a sample SLA constraint could specify that 95% of all SRs from customer 1 with ‘urgent’ priority must be resolved within 4 hours. While the need for SLA constraints to be met is obvious, the requirement for having queues holding unresolved SRs bounded is also necessary because SLA attainments are calculated only for the work completed. The problem is challenging because analytical modeling of SS operations is difficult due to aggregate SLA constraints and also because the SS characteristics such as work patterns, technologies, and customers supported change frequently. An important aspect to consider in the design of the adaptive labor staffing algorithm is its computational efficiency, as an algorithm with low running time helps in making staffing changes on a shorter timescale, for instance, every week.

We formulate this problem as a constrained Markov cost process that depends on the worker parameter. To have a sense of the search space size, an SS consisting of 30 SWs who work in 6 shifts and 3 distinct skill levels corresponds to more than 2 trillion configurations. We design a novel single-stage cost function for the constrained Markov cost process that balances the conflicting objectives of worker under-utilization and SLA under/over-achievement. SLA under-achievement implies violation of the SLA constraint. Whereas worker under-utilization clearly points to suboptimal staffing, SLA over-achievement points to ‘over-delivery’ and hence is also suboptimal. The performance objective is a long-run average of this single stage cost function and the goal is to find the optimum steady state worker parameter (i.e., the one that minimizes this objective) from a discrete high-dimensional parameter set. However, our problem setting also involves constraints relating to queue stability and SLA compliance. Thus, the optimum worker parameter is in fact a constrained minimum. Another difficulty in finding the optimum (constrained) worker parameter is that the single stage cost and constraint functions can be estimated only via simulation. Hence, the need is for a simulation-optimization algorithm that incrementally updates the worker parameter along a descent direction, while adhering to a set of queue stability and SLA constraints.

In this paper, we develop two novel discrete parameter simulation-based optimization algorithms for solving the above problem. Henceforth, we shall refer to these algorithms as *SASOC (Staff Allocation using Stochastic Optimization with Constraints)* algorithms. The core of each of the algorithms is a multi-timescale stochastic approximation scheme that incorporates a random perturbation based algorithm for ‘primal descent’ and couples it with a ‘dual ascent’ scheme for the Lagrange multipliers. The first order algorithm¹ proposes the simultaneous perturbation stochastic approximation (SPSA) based technique for gradient estimation in the primal. We also develop a second order (Newton) methods that estimates the Hessian of the objective function using SPSA and leverages Woodbury’s identity to directly estimate the inverse of the Hessian. Both the SASOC algorithms that we propose are online, incremental and easy to implement. Further, all SASOC algorithms involve a certain generalized smooth projection operator, which is essential to project the continuous-valued worker parameter tuned by SASOC algorithms onto the discrete set. The smoothness is necessary to ensure that the underlying transition dynamics of the constrained Markov cost process is itself smooth (as a function of the continuous-valued parameter) - a critical requirement to prove the convergence of all SASOC algorithms. We evaluate our algorithms on five real-life SS in the data-center management domain. For each of the SS, we collect operational data on work arrival patterns, service times, and contractual SLAs and feed this data into the simulation model of (Banerjee et al. 2011). From the simulation experiments, we observe that our algorithms show overall better performance in comparison with the state-of-the-art OptQuest optimization toolkit ((April et al. 2001)).

¹A part of this work appeared as a short paper in ICSOC 2011 (Prashanth et al. 2011)

Further, our algorithms are 25 times faster than OptQuest and have a significantly lower execution runtime.

1.1 Contributions to theory and methodology

Newton-based algorithms usually suffer from the problem of high per-iterate computational requirement because of the need to estimate the inverse of the Hessian matrix at each update epoch. We propose, for the first time, a method for directly updating the inverse Hessian in Newton-based Simultaneous Perturbation Stochastic Approximation algorithms based on incorporating the Woodbury identity. This is seen to result in significant computational savings as the resulting Newton algorithm shows fast convergence. Our algorithm is based on a novel generalized projection scheme. Since our problem setting is one of discrete constrained optimization, we first transform the problem for purposes of proving convergence (using the proposed generalized projection scheme) to a continuous constrained optimization setting. Note that SPSA is primarily a continuous optimization technique. Our main observation is that SPSA also serves as a powerful method in the context of discrete optimization even when inequality constraints are considered. We prove the convergence of the proposed SPSA algorithms. In the context of discrete optimization problems (with or without inequality constraints) based on simulation, ours is the first work that develops Newton-based search algorithms.

1.2 Contributions to practice

Optimizing staff allocation in the context of service systems is challenging and the problem is further complicated by SLA constraints which are aggregate in nature. Our system model (constrained Markov cost process) incorporates non-stationary workload arrivals and service times whose distribution is fitted from historical data and follows a lognormal (and not exponential) distribution. We present novel simulation optimization algorithms based on simultaneous perturbation technique that solve this problem. The proposed algorithms include both first order as well as second order optimization schemes and attempt to find the optimal staffing levels working with simulated data. Further, the proposed schemes are guaranteed to work with any given dispatching policy. Both our algorithms are online, incremental and computationally efficient - characteristics that make them amenable for their use in real service systems, especially with shorter periodicity for staff changes. From the numerical experiments based on data from real-life service systems, we observe that our SASOC algorithms exhibited overall superior performance in comparison to the state-of-the-art simulation optimization toolkit OptQuest. The experiments were performed with two different dispatching policies and it was observed that in each case SASOC algorithms converged rapidly to solutions of good quality at lower computational overhead as compared to OptQuest.

2 Related Work

We now review literature in two different areas of related work: (1) techniques pertaining to service systems analysis and (2) developments in stochastic optimization approaches.

2.1 Service Systems

In (Verma et al. 2011), a two-step mixed-integer program is formulated for the problem of dispatching SRs within service systems. While their goal is similar to ours, their formulation does not model the stochastic variations in arrivals and service times. Further, unlike our framework, the SLAs in their formulation are not aggregated over a month long period. In (Wasserkrug et al. 2008), the authors propose a scheme for shift-scheduling in the context of third-level IT support systems. Unlike this paper, they do not validate their method against data from real-life third-level IT support. In (Cezik and L'Ecuyer 2008; Bhulai et al.

2008), simulation-optimization methods are proposed for finding the optimal staffing in a multiskill call center, where the constraints are on long-term SLA requirements. While the paper by (Cezik and L'Ecuyer 2008) proposes a cutting plane algorithm for solving an integer program, (Bhulai et al. 2008) relies on obtaining a linear programming solution. However, unlike SASOC algorithms, steady-state system analysis is not performed there. Instead, they solve a sample problem and show that the optimal solution of the sample problem converges to that of the exact problem when the number of samples go to infinity. In (Robbins and Harrison 2008), usage of a simulation based search method is proposed for finding the optimal staffing levels in the context of a call-center domain. They evaluate the system given a staffing level with an analytical model, which is possible in their simplified domain but would not be feasible for service systems due to aggregate SLA constraints and dynamic queues. An analysis of service systems using the ARENA simulation tool is presented in (Brickner et al. 2010). Unlike our model, the system there is not subjected to aggregate SLA constraints and they do not consider preemption of low priority SRs by higher priority SRs and assignment of higher skilled SWs to growing queues of SRs requiring lower skill levels. In (Banerjee et al. 2011), a simulation framework for evaluating dispatching policies is proposed. While we share their simulation model, the goal in this paper is to develop simulation optimization methods for optimizing the worker parameter in a constrained setting. In general, none of the above papers propose an optimization algorithm that is geared for SS and that leverages simulation to adapt optimization search parameters, when both the objective and the constrained functions are suitable long-run averages.

In (Prasad et al. 2013), some algorithms based on the smoothed functional technique for gradient estimation were proposed for the problem of staffing optimization in service systems. The algorithms there used certain random perturbations based on Gaussian and Cauchy density functions to estimate the gradient of the Lagrangian. While we use random perturbations using i.i.d., symmetric, ± 1 -valued, Bernoulli random variables, the computational cost involved in our algorithms is significantly low when compared to (Prasad et al. 2013) because generating Bernoulli distributed random variables is significantly less expensive than generating Gaussian or Cauchy random variates. Further, we also propose second-order Newton based methods, which are more robust than the first order methods in the aforementioned reference. We compare our proposed algorithms with the ones from (Prasad et al. 2013) in the numerical experiments.

2.2 Stochastic Optimization

SPSA ((Spall 1992)) is a popular and highly efficient simulation based local optimization scheme for gradient estimation. SPSA has the critical advantage that it needs only two samples of the objective function to estimate its gradient for any N -dimensional parameter. In (Spall 1997), a one-simulation variant of SPSA was proposed. However, the algorithm in (Spall 1997) was not found to work as well in practice as its two simulation counterpart. Usage of deterministic perturbations instead of randomized was proposed in (Bhatnagar et al. 2003). The deterministic perturbations there were based either on lexicographic or Hadamard matrix generated sequences and were found to perform better than their randomized perturbation counterparts. Another approach that is seen to improve the performance of gradient SPSA is to use a chaotic nonlinear random number generator, see (Bhatnagar and Borkar 2003). A Newton based SPSA algorithm that needs four system simulations with Bernoulli random perturbations was proposed in (Spall 2000). In (Bhatnagar 2005), three other SPSA based estimates of the Hessian that require three, two and one system simulations, respectively, were proposed. In (Bhatnagar 2007), certain smoothed functional (SF) Newton algorithms that incorporate Gaussian-based perturbations were proposed. In (Bhatnagar et al. 2011b) continuous optimization techniques such as SPSA and SF, have been adapted to a setting of discrete parameter optimization. Two simulation based optimization algorithms that involve randomized projections have been proposed there for an unconstrained setting. In (Bhatnagar et al. 2011a), several simulation based algorithms for constrained optimization have been proposed. Two of the algorithms proposed there use SPSA for estimating the gradient, after applying the Lagrange relaxation procedure to the constrained optimization

problem, while the other two incorporate SF approximation. For a detailed survey of gradient estimation techniques in the context of simulation optimization, the reader is referred to (Bhatnagar et al. 2013).

Our SASOC algorithms differ from the stochastic optimization approaches outlined above in various ways. Many algorithms, for instance those proposed in (Spall 2000; Bhatnagar 2005, 2007), are for unconstrained optimization and in a continuous optimization setting. However, our staff optimization problem is for a discrete worker parameter and requires SLA and queue stability constraints to be satisfied in the long-run-average sense. While the algorithms of (Bhatnagar et al. 2011a) have been developed for constrained optimization in the case of a continuously-valued parameter, our SASOC algorithms optimize a discrete parameter. Further, unlike (Bhatnagar et al. 2011a) where an explicit inversion of the Hessian at each update step was advocated, we incorporate the Woodbury’s identity to obtain a novel update step for the inverse of the Hessian in our algorithm SASOC-W. Unlike (Bhatnagar et al. 2011b) where fully randomized projections were used, we incorporate a generalized projection operator that is continuously differentiable in the parameter and works as a deterministic operator over a large portion of the search space and incorporates randomization over a small portion. This helps in bringing down the computational requirement as a deterministic projection scheme requires less computation than a fully randomized one. To the best of our knowledge, we are the first to present adaptations of Newton-based search approaches for constrained discrete optimization problem.

The rest of the paper is organized as follows: First, we present the detailed problem formulation. Second, we introduce our solution methodology and present simultaneous perturbation based SASOC algorithms for adaptive labor staffing. Third, we provide an outline of the convergence proof and state the main results.² Fourth, we discuss the implementation of our algorithms as well as the OptQuest algorithm and present the performance simulation results. Finally, we provide the concluding remarks and discuss interesting future research directions.

3 Problem Formulation

A service system is characterized by the following entities.

- A finite set of customers, denoted by \mathcal{C} , supported by the service system.
- A finite set of shifts, denoted by \mathcal{A} , across which the service workers are distributed.
- A finite set of skill or complexity levels, denoted by \mathcal{B} .
- A finite set of priority levels, denoted by the set P .
- A finite set of time intervals, denoted by \mathcal{I} , where during each interval the arrivals stay stationary, with the number of arrivals following a Poisson distribution whose rate parameter is given by the function α described next.
- Arrival rates specified by the mapping $\sigma : \mathcal{C} \times \mathcal{I} \rightarrow \mathbb{R}$. We assume that each of the SR arrival processes from the various customers C_i are independent and Poisson distributed with $\alpha(C_i, I_j)$ specifying the rate parameter. Owing to the finite-buffer nature of the system, we assume that the number of arrivals during any interval ($\in \mathcal{I}$) is upper-bounded by a sufficiently large constant.
- Service time distributions characterized by the mapping $\tau : P \times \mathcal{B} \rightarrow (r_1, r_2), r_i \in \mathbb{R}, i = 1, 2$. Here r_1 represents the mean and r_2 the standard deviation of a truncated lognormal distributed random variable

²The detailed proofs have been provided for review in a separate document attached to the paper.

Table 1: Sample workers, utilizations and SLA targets

(a) Workers θ_i

Shift	Skill levels		
	High	Med	Low
S1	1	3	7
S2	0	5	2
S3	3	1	2

(b) Utilizations $u_{i,j}$

Shift	Skill levels		
	High	Med	Low
S1	67%	34%	26%
S2	45%	55%	39%
S3	23%	77%	62%

(c) SLA targets $\gamma_{i,j}$

Priority	Customers	
	Bossy Corp	Cool Inc
P_1	95%4h	89%5h
P_2	95%8h	98%12h
P_3	100%24h	95%48h
P_4	100%18h	95%144h

corresponding to a particular priority-complexity pair. In other words, if M is a random variable following a normal distribution with mean r_1 and standard deviation r_2 , then the truncated lognormal random variable is $e^M \wedge \top$, where \top is a truncation constant that is chosen to be large in practice.

- SLA constraints, given by the mapping $\gamma : \mathcal{C} \times \mathcal{P} \rightarrow (r_1, r_2), r_i \in \mathbb{R}, i = 1, 2$. Here $\gamma(C_i, P_j) = (r_1, r_2)$ implies that the SLA target for SRs from customer C_i and with priority P_j is (r_1, r_2) , with r_1 specifying the SLA percentage target and r_2 the resolution time target (in hours). For instance, $\gamma(C_1, P_1) = (95, 4)$ translates to the requirement that at least 95% of the SRs from customer C_1 with priority level P_1 should be closed within 4 hours. Note that the SLAs are computed at the end of each month and hence the aggregate SLA targets are applicable to all SRs that are closed within the month under consideration. Henceforth, we shall adopt the notation $\gamma_{i,j}$ to denote $\gamma(C_i, P_j)$.

Note that each arriving SR has a customer identifier ($\in \mathcal{C}$), a priority identifier ($\in \mathcal{P}$) and a complexity identifier ($\in \mathcal{B}$), whereas any SW works in a particular shift ($\in \mathcal{A}$) and possesses a skill level ($\in \mathcal{B}$). In other words, each customer can issue multiple SRs with their respective SLA targets and the SWs with the right skill level and relevant shift have to pull these SRs from the complexity queues and close them within the deadline specified by the SLA. The set \mathcal{I} and the mapping α allow us to model the variations in arrival rates better than in a setting where the arrivals are assumed to be Poisson-distributed for the entire period. Further, the time taken by an SW to complete an SR is stochastic and follows a lognormal distribution, where the parameters of the distribution are learned by conducting time and motion exercises described in (Banerjee et al. 2011).

Table 1(a) illustrates a simple SS configuration, specifying the staffing levels across shifts and skill levels. This essentially constitutes the worker parameter that we optimize. In this example, $\mathcal{A} = \{S1, S2,$

S3} and $\mathcal{B} = \{\text{high, medium, low}\}$. Tables 1(b) and 1(c) provide sample utilizations and SLA targets on a SS with three shifts, two customers and four priority levels.

Figure 1 shows the main components of the SS. The SRs arrive from multiple customers and the arrival rate is specific to the hour of week, i.e., within each hour of week, and for each customer-priority pair, the arrivals follow a Poisson distribution. The parameters of this distribution are learned from historical data over a period of at least 6 months. Once the SR arrives, it is queued up in a matching complexity queue by the queue manager and the dispatcher would then assign it to an SW based on the dispatching policy. For instance, in the PRIO-PULL policy, SRs are queued in the complexity queues based directly on the priority assigned to them by the customers. On the other hand, in the EDF policy, the time left to SLA target deadline is used to assign the SRs to the SWs i.e., the SW works on the SR that has the earliest deadline. Note that we have a finite buffer system, i.e., the number of SRs in each of the complexity queues is upper-bounded by a sufficiently large constant. Any arriving SR that finds the corresponding complexity queue full will depart the system.

A SW works in exactly one shift (working days and times) and a SS may operate in multiple shifts. We say that a particular configuration of workers across shifts and skill levels is feasible if (a) the SLA constraints are met and (b) the complexity queues do not become unbounded when using this configuration. While the need for (a) is obvious, the requirement for having bounded complexity queues is also necessary. This is because SLA attainments are calculated only for work completed and not for work waiting for completion in the complexity queues. For instance, say in a given month, 100 SRs arrive at various times from a customer to a SS and only 50 of them are completed within the target completion time stipulated by the SLA constraints. The remaining 50 SRs are still in progress without a known completion time and hence do not have an impact on the SLA attainment measures. Thus, a healthy SLA attainment alone is insufficient and the bound on the growth of complexity queues fills the gap.

3.1 Constrained parameterized Markov Cost Process

We consider the setting of a constrained parameterized Markov cost process that we describe in detail below³. Our setting, however, involves a discrete-time, continuous-space Markov process represented by $\{X_n(\theta), n \geq 0\}$. We describe X_n more clearly in Section 3.3. The transition probabilities of this process depend on the worker parameter $\theta = (\theta_1, \dots, \theta_N)^T \in \mathcal{D}$, where $N = |A| \times |B|$. In the above, θ_i indicates the number of service workers whose skill level is $(i-1)\%|B|$ and whose shift index is $(i-1)/|B|$. As an example, the worker parameter for the setting in Table 1(a) is $\theta = (\theta_1, \dots, \theta_9)^T = (1, 3, 7, 0, 5, 2, 3, 1, 2)^T$. The parameter vector θ takes values in the set \mathcal{D} , where $\mathcal{D} \triangleq \{0, 1, \dots, W_{\max}\}^N$. Here W_{\max} serves as an upper bound for the number of workers in any shift and of any skill level. Note that one can enumerate all the points in \mathcal{D} as $\mathcal{D} = \{D^1, D^2, \dots, D^p\}$ for some $p > 1$.

As illustrated in Figure 2, the system stochastically transitions from one state to another, while incurring a state-dependent cost. In addition, there are state-dependent single-stage (constraint) functions described via $g_{i,j}(X_n), h(X_n), i = 1, \dots, |C|, j = 1, \dots, |P|$. These shall correspond to the SLA and queue stability constraints. The state together with the cost and constraint functions constitutes the constrained Markov cost process. The n th system transition of this underlying process involves a simulation of the service system for a fixed period \mathcal{T} with the current worker parameter $\theta(n)$. However, arrivals are stopped after time \mathcal{T} and the service system is simulated until the complexity queues are empty. In our experiments, $\mathcal{T} = 10$, i.e., we simulate the service system for a period of ten months with the staffing levels specified by $\theta(n)$. Also, note that this is a continuously running simulation where, at discrete time instants $n\mathcal{T}$, we update the worker

³A similar framework is considered, for instance, in (Marbach and Tsitsiklis 2001; Prasad et al. 2013). However, the setting considered in (Marbach and Tsitsiklis 2001) is unconstrained and the parameter is continuous-valued. Our formulation, though similar to that in (Prasad et al. 2013), is simpler as it does not involve hidden state components.

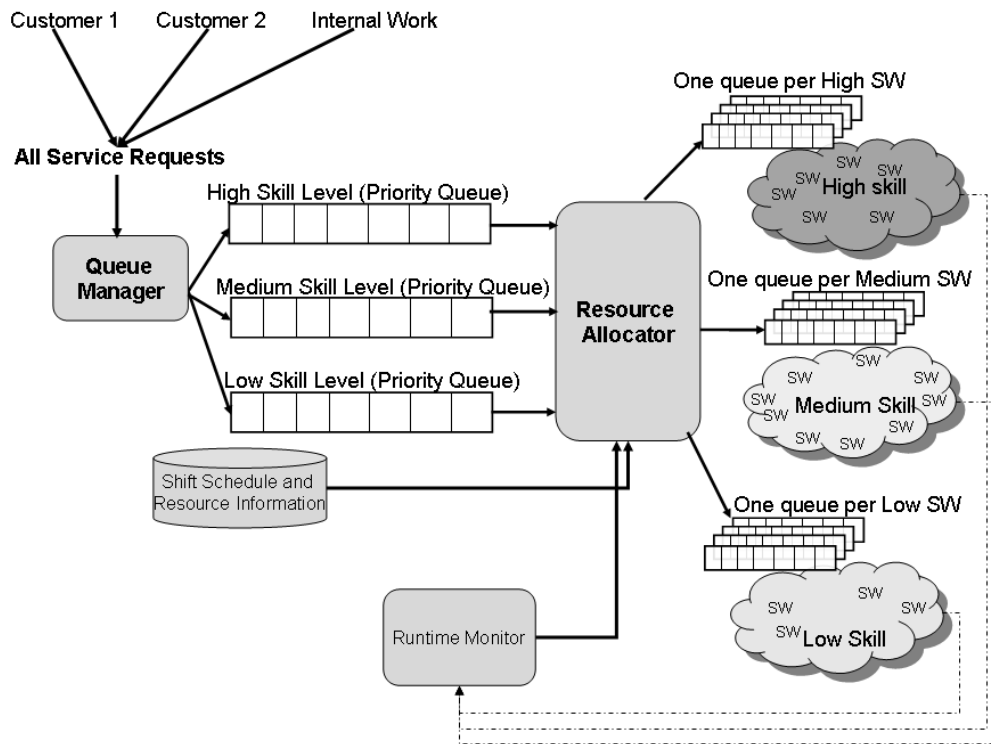


Figure 1: Operational model of an SS

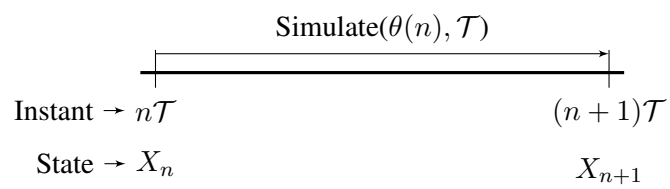


Figure 2: A portion of the time-line illustrating the process

parameter $\theta(n)$ and the simulation output causes a probabilistic transition from the current state X_n to the next state X_{n+1} , while incurring a single-stage cost $c(X_n)$. The precise definitions of the state, the cost and the constraints functions are given in Section 3.3. By an abuse of notation, we refer to the state at instant $n\mathcal{T}$ as X_n .

3.2 The Objective

We use the long-run average cost as the performance objective in our setting. Thus, we are interested in optimizing the steady-state system performance. The optimization problem is the following:

$$\begin{aligned}
& \text{Find } \min_{\theta} J(\theta) \triangleq \lim_{n \rightarrow \infty} \frac{1}{n} \sum_{m=0}^{n-1} c(X_m) \\
& \text{subject to} \\
& G_{i,j}(\theta) \triangleq \lim_{n \rightarrow \infty} \frac{1}{n} \sum_{m=0}^{n-1} g_{i,j}(X_m) \leq 0, \\
& \quad \forall i = 1, \dots, |C|, j = 1, \dots, |P|, \\
& H(\theta) \triangleq \lim_{n \rightarrow \infty} \frac{1}{n} \sum_{m=0}^{n-1} h(X_m) \leq 0.
\end{aligned} \tag{1}$$

We assume below that the Markov process $\{X_n\}$ under any parameter θ is ergodic. In such a case, the limits in (1) are well-defined. If this is not the case, one may replace the “lim” with “limsup” in the definitions of $J(\theta)$, $G_{i,j}(\theta)$ and $H(\theta)$ in (1). Given the above constrained Markov cost process formulation, the optimization problem (1) essentially stipulates that the optimal worker parameter θ^* should minimize the long-run average cost objective $J(\cdot)$ while maintaining queue stability in steady-state (i.e., the long-run average of $h(X_n)$ should not be above zero) and adhering to contractual SLAs, i.e., that the long-run average of $g_{i,j}(X_n)$ should not be above zero, for any feasible (i, j) -tuple.

The SASOC algorithms that we design subsequently (see Section 4) use the cost $c(X_n)$ and constraint functions $g_{i,j}(X_n)$, $h(X_n)$ to tune the worker parameter $\theta(n)$ at instant $n\mathcal{T}$ and the system simulation would now continue with the updated worker parameter. While it is desirable to find the optimum $\theta^* \in S$, i.e.,

$$\theta^* = \operatorname{argmin} \left\{ J(\theta) \text{ s.t. } \theta \in \mathcal{D}, G_{i,j}(\theta) \leq 0, i = 1, \dots, |C|, j = 1, \dots, |P|, H(\theta) \leq 0 \right\},$$

it is in general very difficult to achieve a global minimum. We apply the Lagrange relaxation procedure to the above problem and then provide SPSA based algorithms - both first as well as second order, for finding a locally optimum parameter θ^* . We now describe in detail the state, single-stage cost and constraint functions that we adopt for the constrained Markov cost process formulated for optimizing the staffing in the context of service systems.

3.3 State, Cost and Constraints

The state X_n at instant n is the vector of the length of waiting SR queues corresponding to each skill level, the current utilization of workers for each shift and skill level, and the current SLA attainments for each customer and SR priority. Thus,

$$X_n = (\mathcal{N}(n), u(n), \gamma'(n), q(n)), \tag{2}$$

where,

- $\mathcal{N}(n) = (\mathcal{N}_1(n), \dots, \mathcal{N}_{|B|}(n))^T$, with $\mathcal{N}_i(n)$ being the number of SRs in the system queue corresponding to skill level $i \in \mathcal{B}$. As all the complexity queues are of finite size, we have $\mathcal{N}_i(n) \leq \varsigma, i = 1, \dots, |B|$, where $\varsigma > 0$ is a sufficiently large constant.

- The utilization vector $u(n) = (u_{1,1}(n), \dots, u_{|A|,|B|}(n))$, with each $u_{i,j}(n) \in [0, 1]$ being the average utilization of the workers in shift i and skill level j , at instant n .
- The SLA attainment vector $\gamma'(n) = (\gamma'_{1,1}(n), \dots, \gamma'_{|C|,|P|}(n))$, with $\gamma'_{i,j}(n) \in [0, 1]$ being the SLA attainment for customer i and priority j , at instant n .
- $q(n)$ is an indicator variable that denotes the queue feasibility status of the system at instant n . In other words, $q(n)$ is 0 if the growth rate of the SR queues (for each complexity) is beyond a threshold and is 1 otherwise. We need $q(n)$ to ensure system steady-state which is independent of SLA attainments because the latter are computed only on the SRs that were completed and not on those queued up in the system.

Let S denote the state space. We observe that S is a compact set. This is because each of the state components in X_n take values in sets that are closed and bounded. In particular, each element of $u(n)$, $\gamma'(n)$ takes values in $[0, 1]$ and $0 \leq q(n) \leq 1$, respectively. The system SR queues \mathcal{N} are also of finite length and hence, X_n is bounded.

Considering that the queue lengths, utilizations and SLA attainments at instant $n + 1$ depend only on the state X_n at instant n , we observe that $\{X_n(\theta), n \geq 0\}$ is a constrained Markov cost process for any given (fixed) parameter θ . We now describe in detail the single-stage cost function, whose long-run average sum we try to optimize in (1). We let the cost function $c(X_n)$ have the form:

$$c(X_n) = r \times \left(1 - \sum_{i=1}^{|A|} \sum_{j=1}^{|B|} \alpha_{i,j} \times u_{i,j}(n)\right) + s \times \left(\frac{\sum_{i=1}^{|C|} \sum_{j=1}^{|P|} |\gamma'_{i,j}(n) - \gamma_{i,j}|}{|C| \times |P|}\right), \quad (3)$$

where $r, s \geq 0$ and $r + s = 1$. Further, $0 \leq \gamma_{i,j} \leq 1$ denotes the contractual SLA for customer i and priority j . The single-stage cost function here is a linear function of the state and remains bounded. In fact, from (3), we observe that $0 \leq c(X_n) \leq 1$. This is because $u_{i,j}(n), \gamma_{i,j}, \gamma'_{i,j}(n) \in [0, 1]$ and each component in (3) is upper-bounded by 1.

The cost function is designed to balance between two conflicting objectives of maximizing the utilization of workers and meeting the SLA requirements simultaneously. By the first component in (3), we seek to minimize the under-utilization of workers as it is more fine-grained and hence, allows tighter minimization in comparison to minimizing just the sum of workers across shifts and skill levels. The second component in (3) represents the over/under-achievement of SLAs, which is the distance between attained and the contractual SLAs. While the need for meeting the target SLAs motivates the under-achievement part in the second component, it is also necessary to minimize over-achievement of SLAs. This is because an over-achieved SLA, for instance meeting 100% instead of the target of 95% for a particular customer, while being desirable for the customer, requires more time and effort from some of the workers and does not bring in additional rewards.

Note that the first term in (3) uses a weighted sum of utilizations over workers from each shift and across each skill level. Further, the weights $\alpha_{i,j}$ are fixed and not time-varying. Using historical data on SR arrivals, the percentage of workload arriving in each shift and for each skill level is obtained. These percentages decide the weights $\alpha_{i,j}$ used in (3), that in turn satisfy

$$0 \leq \alpha_{i,j} \leq 1, \text{ and } \sum_{i=1}^{|A|} \sum_{j=1}^{|B|} \alpha_{i,j} = 1,$$

for $i = 1, 2, \dots, |A|$, and $j = 1, 2, \dots, |B|$. This prioritization of workers helps in optimizing the worker set based on the given workload. For instance, if 70% of the SRs requiring low skill worker attention arrive in shift 1, then one may set $\alpha_{1,0} = 0.7$, in the cost function (3), where 0 denotes the low skill level index.

The single-stage constraint functions $g_{i,j}(\cdot), h(\cdot), i = 1, \dots, |C|, j = 1, \dots, |P|$, are given by:

$$g_{i,j}(X_n) = \gamma_{i,j} - \gamma'_{i,j}(n), \forall i = 1, \dots, |C|, j = 1, \dots, |P|, \quad (4)$$

$$h(X_n) = 1 - q(n). \quad (5)$$

Here (4) specifies that the attained SLA levels should be equal to or above the contractual SLA levels for each customer-priority tuple. Further, (5) ensures that the SR queues for each complexity in the system stay bounded. In the constrained optimization problem formulated below, we attempt to satisfy these constraints in the long-run average sense (see (1)).

The SASOC algorithms treat the parameter as continuous-valued and tune it accordingly. Let us denote this continuous version of the worker parameter by $\bar{\theta} = (\bar{\theta}_1, \dots, \bar{\theta}_N)$. Note that $\bar{\theta}_i \in [0, W_{\max}], i = 1, 2, \dots, N$. We now design a smooth projection operator Γ that projects $\bar{\theta}$ on to the discrete space \mathcal{D} so that the same can be used for performing the simulation of the service system. We call the Γ -operator as a generalized projection scheme as it lies in between a fully deterministic projection scheme based on mere rounding off and a completely randomized scheme, whereby depending on the value of $\bar{\theta}_j$ (for any $j = 1, \dots, N$) one can find points \mathcal{D}^k and \mathcal{D}^{k+1} with $\mathcal{D}^k < \mathcal{D}^{k+1}$, $\mathcal{D}^k, \mathcal{D}^{k+1} \in \mathcal{D}$ such that \mathcal{D}^k and \mathcal{D}^{k+1} are the immediate neighbours of $\bar{\theta}_j$ in the set \mathcal{D} . Then, one sets the corresponding discrete parameter as

$$\theta_j = \begin{cases} \mathcal{D}^{k+1} & \text{w.p. } \frac{\bar{\theta}_j - \mathcal{D}^k}{\mathcal{D}^{k+1} - \mathcal{D}^k}, \\ \mathcal{D}^k & \text{w.p. } \frac{\mathcal{D}^{k+1} - \bar{\theta}_j}{\mathcal{D}^{k+1} - \mathcal{D}^k}, \end{cases} \quad (6)$$

where, w.p. stands for ‘with probability’.

3.4 A Generalized Projection Operator

For any $\bar{\theta} = (\bar{\theta}_1, \dots, \bar{\theta}_N)$ with $\bar{\theta}_j \in [0, W_{\max}], j = 1, 2, \dots, N$, we define a projection operator $\Gamma(\bar{\theta}) = (\Gamma_1(\bar{\theta}_1), \dots, \Gamma_N(\bar{\theta}_N)) \in \mathcal{D}$ which projects any $\bar{\theta}$ onto the discrete set \mathcal{D} as follows:

For convenience, lets enumerate the elements of \mathcal{D} as $\mathcal{D} = \{\mathcal{D}^1, \mathcal{D}^2, \dots, \mathcal{D}^p\}$ for some $p > 1$. Let $\zeta > 0$ be a fixed real number and $\bar{\theta}_i$ be such that $\mathcal{D}^j \leq \bar{\theta}_i \leq \mathcal{D}^{j+1}, \mathcal{D}^j < \mathcal{D}^{j+1}$ for some $\mathcal{D}^j, \mathcal{D}^{j+1} \in \mathcal{D}$. Let us consider an interval of length 2ζ around the midpoint of $[\mathcal{D}^j, \mathcal{D}^{j+1}]$ and denote it as $[\tilde{\mathcal{D}}_1, \tilde{\mathcal{D}}_2]$, where $\tilde{\mathcal{D}}_1 = \frac{\mathcal{D}^j + \mathcal{D}^{j+1}}{2} - \zeta$ and $\tilde{\mathcal{D}}_2 = \frac{\mathcal{D}^j + \mathcal{D}^{j+1}}{2} + \zeta$. Then, $\Gamma_i(\bar{\theta}_i)$ for $\theta_i \in [\mathcal{D}^j, \tilde{\mathcal{D}}_1] \cup [\tilde{\mathcal{D}}_2, \mathcal{D}^{j+1}]$ is defined by

$$\Gamma_i(\bar{\theta}_i) = \begin{cases} 0 & \text{if } \bar{\theta}_i < 0 \\ \mathcal{D}^j & \text{if } \bar{\theta}_i \leq \frac{\mathcal{D}^j + \mathcal{D}^{j+1}}{2} - \zeta \\ \mathcal{D}^{j+1} & \text{if } \bar{\theta}_i \geq \frac{\mathcal{D}^j + \mathcal{D}^{j+1}}{2} + \zeta \\ W_{\max} & \text{if } \bar{\theta}_i \geq W_{\max}. \end{cases} \quad (7)$$

Further, $\Gamma_i(\bar{\theta}_i)$ for $\bar{\theta}_i \in [\tilde{\mathcal{D}}_1, \tilde{\mathcal{D}}_2]$ is given by

$$\Gamma_i(\bar{\theta}_i) = \begin{cases} \mathcal{D}^j & \text{w.p. } f\left(\frac{\tilde{\mathcal{D}}_2 - \bar{\theta}_i}{2\zeta}\right) \\ \mathcal{D}^{j+1} & \text{w.p. } 1 - f\left(\frac{\tilde{\mathcal{D}}_2 - \bar{\theta}_i}{2\zeta}\right) \end{cases} \quad (8)$$

In the above, f is any continuously differentiable function defined on $[0, 1]$ such that $f(0) = 0$ and $f(1) = 1$. Note that we deterministically project onto either \mathcal{D}^j or \mathcal{D}^{j+1} if $\bar{\theta}_i$ is outside of the interval $[\tilde{\mathcal{D}}_1, \tilde{\mathcal{D}}_2]$. Further, for $\bar{\theta}_i \in [\tilde{\mathcal{D}}_1, \tilde{\mathcal{D}}_2]$, we project randomly using a smooth function f . It is necessary to have a

smooth projection operator to ensure convergence of our SASOC algorithms as opposed to a deterministic projection operator that would project $\bar{\theta}_i \in [\mathcal{D}^j, \frac{\mathcal{D}^j + \mathcal{D}^{j+1}}{2})$ to \mathcal{D}^j and $\bar{\theta}_i \in [\frac{\mathcal{D}^j + \mathcal{D}^{j+1}}{2}, \mathcal{D}^{j+1}]$ to \mathcal{D}^{j+1} . The problem with a deterministic projection operator is that there is a jump at the midpoint of the interval and hence, when extended for any θ in the convex hull $\bar{\mathcal{D}}$, the transition dynamics of the process $\{X_n, n \geq 0\}$ is not continuously differentiable. A non-smooth projection operator makes the dynamics non-smooth at the boundary points.

The SASOC algorithms that we present subsequently tune the worker parameter in the convex hull of \mathcal{D} , denoted by $\bar{\mathcal{D}}$, a set that can be defined as $\bar{\mathcal{D}} = [0, W_{\max}]^N$. This idea has been used in (Bhatnagar et al. 2011b) for an unconstrained discrete optimization problem. However, the projection operator used there was a fully randomized operator. The generalized projection scheme that we incorporate has the advantage that while it ensures that the transition dynamics of the parameter extended Markov process is smooth (as desired), it requires a lower computational effort because in a large portion of the parameter space (assuming ζ is small), the projection operator is essentially deterministic.

We also require another projection operator $\bar{\Gamma}$ that projects any $\theta \in \mathbb{R}^N$ onto the set $\bar{\mathcal{D}}$ and is defined as $\bar{\Gamma}(\theta) = (\bar{\Gamma}_1(\theta_1), \dots, \bar{\Gamma}_N(\theta_N))$, where $\bar{\Gamma}_i(\theta_i) = \min(0, \max(\theta_i, W_{\max}))$, $i = 1, \dots, N$. Thus, $\bar{\Gamma}(\cdot)$ keeps the parameter updates within the set $\bar{\mathcal{D}}$ and $\Gamma(\cdot)$ projects them to the discrete set \mathcal{D} . The projected updates are then used as the parameter values for conducting the simulation of the service system.

3.5 Assumptions

We now make the following standard assumptions: One amongst (A2) and (A2') will be assumed for the algorithms that follow.

- (A1) The Markov process $\{X_n(\theta), n \geq 0\}$ under a given dispatching policy and parameter θ is ergodic.
- (A2) The single-stage cost functions $c(\cdot)$, $g_{i,j}(\cdot)$ and $h(\cdot)$ are all continuous. The long-run average cost $J(\cdot)$ and constraint functions $G_{i,j}(\cdot)$, $H(\cdot)$ are twice continuously differentiable with bounded third derivative.
- (A2') The single-stage cost functions $c(\cdot)$, $g_{i,j}(\cdot)$ and $h(\cdot)$ are all continuous. The long-run average cost $J(\cdot)$ and constraint functions $G_{i,j}(\cdot)$, $H(\cdot)$ are continuously differentiable with bounded second derivative.
- (A3) The step-sizes $\{a(n)\}$, $\{b(n)\}$ and $\{d(n)\}$ satisfy

$$\sum_n a(n) = \sum_n b(n) = \sum_n d(n) = \infty; \sum_n (a^2(n) + b^2(n) + d^2(n)) < \infty,$$

$$\frac{b(n)}{d(n)}, \frac{a(n)}{b(n)} \rightarrow 0 \text{ as } n \rightarrow \infty.$$

Assumption (A1) ensures that the process $\{X_n\}$ is stable for any given θ and ensures that the long-run averages of the single stage cost and constraint functions in (1) are well-defined. As stated earlier, we require one of (A2) and (A2') for our various algorithms. More specifically, (A2) will be assumed for Hessian based schemes, while (A2') will be assumed for gradient approaches. (A2) and (A2') are technical requirements needed to push through suitable Taylor's arguments in order to prove the convergence of the algorithms. The first two conditions in (A3) are standard requirements for step-size sequences and the last condition there ensures a separation of time scales between the different recursions in SASOC algorithms discussed in detail in Section 4.

Remark 1 *As seen before, the state space S is compact and ergodicity of the underlying Markov process $\{X_n\}$ will follow if one ensures that there is at least one worker for each complexity class.*

4 Our algorithms

The constrained long-run average cost optimization problem (1) can be expressed using the standard Lagrange multiplier theory as an unconstrained optimization problem given below.

$$\begin{aligned} \max_{\lambda} \min_{\theta} L(\theta, \lambda) &\triangleq \lim_{n \rightarrow \infty} \frac{1}{n} \sum_{m=0}^{n-1} E \left\{ c(X_m) + \sum_{i=1}^{|C|} \sum_{j=1}^{|P|} \lambda_{i,j} g_{i,j}(X_m) + \lambda_f h(X_m) \right\} \\ &= J(\theta) + \sum_{i=1}^{|C|} \sum_{j=1}^{|P|} \lambda_{i,j} G_{i,j}(\theta) + \lambda_f H(\theta), \end{aligned} \quad (9)$$

where $\lambda_{i,j} \geq 0$, $\forall i = 1, \dots, |C|, j = 1, \dots, |P|$ represent the Lagrange multipliers corresponding to constraints $g_{i,j}(\cdot)$ and λ_f represents the Lagrange multiplier for the constraint $h(\cdot)$, in the optimization problem (1). Also, $\lambda = (\lambda_{i,j}, \lambda_f, i = 1, \dots, |C|, j = 1, \dots, |P|)^T$. The function $L(\theta, \lambda)$ is commonly referred to as the Lagrangian. An optimal (θ^*, λ^*) is a saddle point for the Lagrangian, i.e., $L(\theta, \lambda^*) \geq L(\theta^*, \lambda^*) \geq L(\theta^*, \lambda), \forall \theta, \forall \lambda$. Thus, it is necessary to design an algorithm which descends in θ and ascends in λ in order to find the optimum point. The simplest iterative procedure for this purpose would use the gradients of the Lagrangian with respect to θ and λ to descend and ascend respectively. However, for the given system, the computation of gradient with respect to θ would be intractable due to lack of a closed form expression of the Lagrangian. Thus, a simulation based algorithm is required. The above explanation suggests that an algorithm for computing an optimal (θ^*, λ^*) would need three stages in each of its iterations.

1. The inner-most stage which performs one or more simulations over several time steps and aggregates data, i.e., does the averaging of the single-stage cost and constraint functions $c(\cdot), g_{i,j}(\cdot)$ and $h(\cdot)$ for any given θ and λ updates.
2. The next outer stage which estimates the gradient of the Lagrangian along θ and updates θ along a descent direction. This stage would perform several iterations for a given λ and find a good estimate of θ ; and
3. The outer-most stage which updates the Lagrange multipliers λ along an ascent direction, using the converged values of the inner two loops.

The above three steps will have to be performed iteratively till the solution converges to a saddle point described previously. Note that the loops are nested in the sense that the loop in iteration (1) would be a sub-loop for iteration (2). Likewise, iteration (2) would be a sub-loop for iteration (3). Thus, in between two successive updates of an outer loop (iterations (2) or (3)), one would potentially have to wait for a long time for convergence of the inner loop procedure (iteration (1) or iterations (1) and (2), respectively). This problem gets addressed by using simultaneous updates to all three stages in a stochastic recursive scheme but with different step-size schedules, the outer-most having the smallest while the inner-most having the largest of step-sizes. The resulting scheme is a multiple time-scale stochastic approximation algorithm (Borkar 2008, Chapter 6).

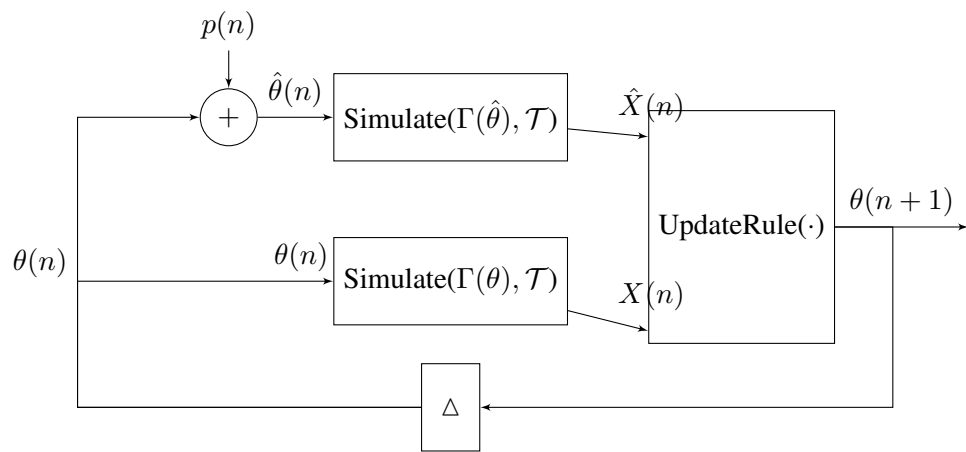


Figure 3: Overall flow of the algorithm 1.

Algorithm 1 Skeleton of SASOC algorithms

Input:

- R , a large positive integer;
- θ_0 , initial parameter vector; $p(\cdot)$; Δ ; $K \geq 1$
- UpdateRule(), the algorithm-specific update rule for the worker parameter θ and Lagrange multiplier λ .
- Simulate(θ, \mathcal{T}) $\rightarrow X$, the simulator of the SS

Output: $\theta^* \triangleq \Gamma(\theta(R))$.

 $\theta \leftarrow \theta_0, n \leftarrow 1$ **loop**Observe $\hat{J}^\theta \leftarrow \text{Simulate}(\Gamma(\theta(n)), \mathcal{T})$. $\hat{X} \leftarrow \text{Simulate}(\Gamma(\theta(n) + p(n)), \mathcal{T})$.

UpdateRule().

 $n \leftarrow n + 1$ **if** $n = R$ **then** Terminate and output $\Gamma(\theta(R))$.**end if****end loop**

The overall flow of all SASOC algorithms can be diagrammatically represented as in Figure 3. Each iteration of the algorithm involves two simulations (each for a period \mathcal{T}) - one with $\Gamma(\theta(n))$, i.e., the current estimate of the parameter projected using the generalized projection operator so that it takes values in the discrete set \mathcal{D} and the other with the (projected) perturbed parameter, $\Gamma(\theta(n)+p(n))$, where the perturbation $p(n)$ is algorithm-specific. For instance, in the case of SASOC-G, $p(n) = \delta\Delta(n)$ and for SASOC-H/W, $p(n) = \delta_1\Delta(n) + \delta_2\hat{\Delta}(n)$, respectively. The rationale behind the choice of $p(n)$ will be subsequently clarified when the individual SASOC algorithms are presented. In every stage of SASOC algorithms, the two simulations are carried out as shown in Figure 3. Using the state values of the two simulations, $X(n)$ and $\hat{X}(n)$, the worker parameter θ is updated in an algorithm-specific manner. Algorithm 1 gives the structure of all three of our incremental update SASOC algorithms.

4.1 SASOC-G Algorithm

SASOC-G is a three time-scale stochastic approximation algorithm that does primal descent using a two-measurement SPSA while performing dual ascent on the Lagrange multipliers.

4.1.1 SPSA based gradient estimate

Here, the gradient of the Lagrangian w.r.t. θ is obtained according to

$$\nabla_{\theta}L(\theta, \lambda) = \lim_{\delta \downarrow 0} E \left[\left(\frac{L(\theta + \delta\Delta, \lambda) - L(\theta, \lambda)}{\delta} \right) \Delta^{-1} \right], \quad (10)$$

where Δ is a vector (of the same dimension as θ) of perturbation random variables that are independent, zero-mean, \pm -valued and have the symmetric Bernoulli distribution. More general distributions on these random variables can be chosen as described in (Spall 1992, 2000). In (10), Δ^{-1} represents element-wise inverse of the Δ vector. This is a one-sided estimate whose convergence is shown in (Chen et al. 1999, Lemma 1).

4.1.2 Update rule of SASOC-G

From the form of the gradient estimator, it is clear that the Lagrangian function would be needed to compute the gradient estimate. However, for our problem, obtaining a closed-form expression for the Lagrangian itself is an intractable task. We overcome this by running two simulations with parameters $\Gamma(\theta(n))$ and $\Gamma(\theta(n) + p(n))$. Here, $p(n) = \delta\Delta(n)$, a choice motivated by the form of the gradient estimate in (10). Using the output of the two simulations, we estimate the quantities $L(\theta + \delta\Delta, \lambda)$ and $L(\theta, \lambda)$, respectively, on the faster timescale. These estimates are in turn used to tune the worker parameter θ in the negative gradient descent direction. For $\lambda_{i,j}$ and λ_f , values of $g_{i,j}(\cdot)$ and $h(\cdot)$ respectively provide a stochastic ascent direction, proof of which will be given later in Theorem 11. Since maximization of the Lagrangian w.r.t. $\lambda_{i,j}$ and λ_f represents the outer-most step, these parameters are updated on the slowest time-scale. The overall

update rule for this scheme, SASOC-G, is as follows: For all $n \geq 0$,

$$\left. \begin{aligned}
\theta_i(n+1) &= \bar{\Gamma}_i \left(\theta_i(n) + b(n) \left(\frac{\bar{L}(nK) - \bar{L}'(nK)}{\delta \Delta_i(n)} \right) \right), \forall i = 1, 2, \dots, N, \\
\text{where for } m &= 0, 1, \dots, K-1, \\
\bar{L}(nK+m+1) &= \bar{L}(nK+m) + \\
& d(n) \left(c(X_{nK+m}) + \sum_{i=1}^{|C|} \sum_{j=1}^{|P|} \lambda_{i,j}(nK) g_{i,j}(X_{nK+m}) + \lambda_f h(X_{nK+m}) - \bar{L}(nK+m) \right), \\
\bar{L}'(nK+m+1) &= \bar{L}'(nK+m) + \\
& d(n) \left(c(\hat{X}_{nK+m}) + \sum_{i=1}^{|C|} \sum_{j=1}^{|P|} \lambda_{i,j}(nK) g_{i,j}(\hat{X}_{nK+m}) + \lambda_f h(\hat{X}_{nK+m}) - \bar{L}'(nK+m) \right), \\
\lambda_{i,j}(n+1) &= (\lambda_{i,j}(n) + a(n) g_{i,j}(X_n))^+, \forall i = 1, 2, \dots, |C|, j = 1, 2, \dots, |P|, \\
\lambda_f(n+1) &= (\lambda_f(n) + a(n) h(X_n))^+.
\end{aligned} \right\} \quad (11)$$

In the above,

- $K \geq 1$ is a fixed parameter which controls the rate of update of θ in relation to that of \bar{L} and \bar{L}' . This parameter allows for accumulation of updates to \bar{L} and \bar{L}' for K iterations in between two successive θ updates;
- X_m represents the state at iteration m from the simulation run with nominal parameter $\Gamma(\theta_{\lfloor \frac{n}{K} \rfloor})$ while \hat{X}_m represents the state at iteration m from the simulation run with perturbed parameter $\Gamma(\theta_{\lfloor \frac{n}{K} \rfloor} + \delta \Delta_{\lfloor \frac{n}{K} \rfloor})$. Here $\lfloor \frac{n}{K} \rfloor$ denotes the integer portion of $\frac{n}{K}$. For simplicity, hereafter we use θ to denote $\theta_{\lfloor \frac{n}{K} \rfloor}$ and $\theta + \delta \Delta$ to denote $\theta_{\lfloor \frac{n}{K} \rfloor} + \delta \Delta_{\lfloor \frac{n}{K} \rfloor}$;
- $\delta > 0$ is a fixed perturbation control parameter while Δ is a vector of perturbation random variables that are independent, zero-mean and have the symmetric Bernoulli distribution;
- The operator $\bar{\Gamma}(\cdot)$ ensures that the updated value for θ stays within the convex hull $\bar{\mathcal{D}}$ and is defined in Section 3.4; and
- \bar{L} and \bar{L}' represent Lagrange estimates corresponding to θ and $\theta + \delta \Delta$ respectively.

We achieve separation of time-scales between the recursions of $\theta_i, \bar{L}, \bar{L}'$ and λ via the difference in the step-sizes $a(n), b(n)$ and $d(n)$ (see (A3)). The chosen step-sizes ensure that the recursions of Lagrange multipliers $\lambda_{i,j}$ proceed ‘slower’ in comparison to those of the worker parameter θ , while the updates of the average cost - \bar{L} and \bar{L}' proceed the fastest.

4.2 SASOC-H Algorithm

This is a second-order algorithm for adaptive labour staffing which uses SPSA based techniques to estimate both the gradient and the Hessian. As discussed before, the overall algorithm structure is represented by Figure 3 with $p(n) = \theta(n) + \delta_1 \Delta(n) + \delta_2 \hat{\Delta}(n)$ in this case. Thus, each iteration of the algorithm involves two simulations (each for a period \mathcal{T}) - one with $\Gamma(\theta(n))$ and the other with $\Gamma(\theta(n) + \delta_1 \Delta(n) + \delta_2 \hat{\Delta}(n))$ as the respective parameters in the n th iteration cycle. As explained in the next section, the two perturbation sequences Δ and $\hat{\Delta}$ are used to estimate both the gradient and the Hessian of the Lagrangian w.r.t. θ .

4.2.1 SPSA based simultaneous estimates for the gradient and the Hessian

Suppose the Lagrangian in (9) is twice differentiable w.r.t. θ , then we can look at possible second order schemes for computing updates to θ . If the Lagrangian (9) were a quadratic, then the exact solution for the θ update to reach the minimum point would have been $-\left[\nabla_{\theta}^2 L(\theta_0)\right]^{-1} \nabla_{\theta} L(\theta_0)$ with θ_0 as the starting point, i.e.,

$$\theta^* = \theta_0 - \left[\nabla_{\theta}^2 L(\theta_0)\right]^{-1} \nabla_{\theta} L(\theta_0),$$

would be the optimal parameter. For a higher-degree Lagrangian, the above solution can be used with a step-size parameter iteratively till convergence to an optimal θ^* . Let Δ and $\widehat{\Delta}$ be two independent vectors of perturbation random variables that are independent, zero-mean, ± 1 -valued and have the symmetric Bernoulli distribution. More general distributions for Δ and $\widehat{\Delta}$ may however be used, see (Spall 1992, 2000). We use the following estimates for the gradient and Hessian, respectively, as described in (Bhatnagar et al. 2011a, Section 3.2.1):

$$\begin{aligned} \nabla_{\theta} L(\theta, \lambda) &= \lim_{\delta_1, \delta_2 \downarrow 0} E \left[\left(\frac{L(\theta + \delta_1 \Delta + \delta_2 \widehat{\Delta}, \lambda) - L(\theta, \lambda)}{\delta_2} \right) \widehat{\Delta}^{-1} \right], \\ \nabla_{\theta}^2 L(\theta, \lambda) &= \lim_{\delta_1, \delta_2 \downarrow 0} E \left[\Delta^{-1} \left(\frac{L(\theta + \delta_1 \Delta + \delta_2 \widehat{\Delta}, \lambda) - L(\theta, \lambda)}{\delta_1 \delta_2} \right) (\widehat{\Delta}^{-1})^T \right], \end{aligned}$$

where Δ^{-1} and $\widehat{\Delta}^{-1}$ represent vectors of element-wise inverses of the Δ and $\widehat{\Delta}$ vectors respectively. Thus, the inner terms of the above two expectations can be used for estimating the Hessian and also updating θ .

4.2.2 Update rule of SASOC-H

For $n \geq 0$, we have

$$\theta_i(n+1) = \bar{\Gamma}_i \left(\theta_i(n) + b(n) \sum_{j=1}^N M_{i,j}(n) \left(\frac{\bar{L}(nK) - \bar{L}'(nK)}{\delta_2 \widehat{\Delta}_j(n)} \right) \right), \quad (12)$$

$$H_{i,j}(n+1) = H_{i,j}(n) + b(n) \left(\frac{\bar{L}'(nK) - \bar{L}(nK)}{\delta_1 \Delta_j(n) \delta_2 \widehat{\Delta}_i(n)} - H_{i,j}(n) \right), \quad (13)$$

for $i, j = 1, \dots, N$. Note that

- The update equations corresponding to \bar{L} , \bar{L}' , $\lambda_{i,j}$, $i = 1, \dots, |C|$, $j = 1, \dots, |P|$ and λ_f are the same as in SASOC-G (11). However, note that the perturbed parameter in this case is $(\theta(n) + \delta_1 \Delta(n) + \delta_2 \widehat{\Delta}(n))$. Thus, unlike SASOC-G, \hat{X}_m represents the state at iteration m from the simulation run with perturbed parameter $\Gamma(\theta(n) + \delta_1 \Delta(n) + \delta_2 \widehat{\Delta}(n))$, while X_m continues to have the same interpretation as with SASOC-G.
- $\delta_1, \delta_2 > 0$ are fixed perturbation control parameters while Δ and $\widehat{\Delta}$ are two independent vectors of perturbation random variables that are independent, zero-mean, ± 1 -valued, and have the symmetric Bernoulli distribution;
- $H = [H_{i,j}]_{i=1, j=1}^{|A| \times |B|, |A| \times |B|}$ represents the Hessian (second-derivative w.r.t. θ) estimate of the Lagrangian. $H(0)$ is a positive definite and symmetric matrix. We let $H(0) = \omega I$, with $\omega > 0$ and I being the identity matrix; and

- $M(n) = \Upsilon(H(n))^{-1} = [M(n)_{i,j}]_{i=1,j=1}^{|A| \times |B|, |A| \times |B|}$ represents the inverse of the Hessian estimate H of the Lagrangian, where $\Upsilon(\cdot)$ is a projection operator ensuring that the Hessian estimates remain symmetric and positive definite. The Υ operation is assumed to satisfy assumption (A4).

Assumption (A4)

The projection operator $\Upsilon(\cdot)$ projects a square matrix to a symmetric positive definite matrix. If $\{A_n\}$ and $\{B_n\}$ are sequences of matrices in $\mathcal{R}^{N \times N}$ such that $\lim_{n \rightarrow \infty} \|A_n - B_n\| = 0$, then $\lim_{n \rightarrow \infty} \|\Upsilon(A_n) - \Upsilon(B_n)\| = 0$ as well. Further, for any sequence $\{C_n\}$ of matrices in $\mathcal{R}^{N \times N}$, if $\sup_n \|C_n\| < \infty$, then $\sup_n \|\Upsilon(C_n)\| < \infty$ and $\sup_n \|\{\Upsilon(C_n)\}^{-1}\| < \infty$, as well.

4.3 Efficient implementation of SASOC-H

The SASOC-H algorithm is more robust than SASOC-G. However, it requires computation of the inverse of the Hessian H at each stage which is a computationally intensive operation. We propose an enhancement using Woodbury's identity to the previous algorithm that results in significant computational gains. In particular, an application of Woodbury's identity brings down the computational complexity from $O(n^3)^4$ to $O(n^2)$ where $n = |A| \times |B|$.

4.3.1 Woodbury's Identity based Update for Hessian Inverse

Woodbury's identity states that

$$(A + BCD)^{-1} = A^{-1} - A^{-1}B(C^{-1} + DA^{-1}B)^{-1}DA^{-1}$$

where A and C are invertible square matrices and B and D are rectangular matrices of appropriate sizes. The Hessian update in (12) without projection can be rewritten as

$$H(n+1) = (1 - b(n))H(n) + P(n)Z(nK)Q(n)$$

where

$$P(n) = \frac{1}{\delta_1} \left[\frac{1}{\Delta_1(n)}, \frac{1}{\Delta_2(n)}, \dots, \frac{1}{\Delta_{|A| \times |B|}(n)} \right]^T, Q(n) = \frac{1}{\delta_2} \left[\frac{1}{\widehat{\Delta}_1(n)}, \frac{1}{\widehat{\Delta}_2(n)}, \dots, \frac{1}{\widehat{\Delta}_{|A| \times |B|}(n)} \right], \text{ and}$$

$$Z(nK) = b(n) (\bar{L}'(nK) - \bar{L}(nK)).$$

Now, applying the Woodbury's identity to $H(n+1)^{-1} = M(n+1)$ gives us the following update:

$$M(n+1) = \left(\frac{M(n)}{1 - b(n)} \left[I - \frac{b(n) (\bar{L}'(nK) - \bar{L}(nK)) P(n) Q(n) M(n)}{1 - b(n) + b(n) (\bar{L}'(nK) - \bar{L}(nK)) Q(n) M(n) P(n)} \right] \right),$$

which is a recursive update rule for directly updating the matrix $M(n)$, which is the inverse of $H(n)$, $n \geq 0$.

The modified update scheme of SASOC-H after incorporating the Woodbury's identity for estimating the inverse of the Hessian, is as follows: For $n \geq 0$,

$$\theta_i(n+1) = \bar{\Gamma}_i \left(\theta_i(n) + b(n) \sum_{j=1}^N M_{i,j}(n) \left(\frac{\bar{L}(nK) - \bar{L}'(nK)}{\delta_1 \widehat{\Delta}_j(n)} \right) \right), \quad (14)$$

$$M(n+1) = \Upsilon \left(\frac{M(n)}{1 - b(n)} \left[I - \frac{b(n) (\bar{L}'(nK) - \bar{L}(nK)) P(n) Q(n) M(n)}{1 - b(n) + b(n) (\bar{L}'(nK) - \bar{L}(nK)) Q(n) M(n) P(n)} \right] \right).$$

⁴The popular Gauss-Jordan procedure for matrix inverse of a matrix requires $O(n^3)$ computations.

In the above, $M(0)$ is initialized to ωI , I being an identity matrix and $\omega > 0$. The rest of the update rule corresponding to \bar{L} , \bar{L}' , $\lambda_{i,j}$, $i = 1, \dots, |C|$, $j = 1, \dots, |P|$ and λ_f are the same as before (see (11)–(12)).

Our SASOC algorithms differ from the algorithms of (Bhatnagar et al. 2011a) in the following ways:

- (i) Unlike the algorithms of (Bhatnagar et al. 2011a) which are for a continuous-valued parameter, our SASOC algorithms are for a constrained discrete optimization setting and involve a generalized projection operator that renders the transition probabilities of the extended Markov process for any $\theta \in \bar{\mathcal{D}}$ smooth.
- (ii) Since the SASOC-W algorithm does not involve explicit computation of the Hessian inverse, it is computationally more efficient than the second-order algorithms of (Bhatnagar et al. 2011a).

5 Notes on convergence

Here we provide a sketch of the convergence of SASOC-G and SASOC-H algorithms.⁵

Step 1: Extension of the transition dynamics $p_{i,j}(\theta)$

The first step in the convergence analysis is common to both the SASOC algorithms and involves the extension of the transition dynamics $p_\theta(i, j)$ of the constrained parameterized Markov process to the convex hull $\bar{\mathcal{D}}$.

Recall that the discrete parameter θ of the Markov process $\{X_n(\theta)\}$ takes values in the set \mathcal{D} defined earlier. Using the members of \mathcal{D} , one can extend the transition dynamics $p_\theta(i, j)$ of the underlying Markov process to any θ in the convex hull $\bar{\mathcal{D}}$ as follows:

$$p_\theta(i, j) = \sum_{k=1}^p \beta_k(\theta) p_{D^k}(i, j), \quad \forall \theta \in \bar{\mathcal{D}}, i, j \in S, \quad (15)$$

where the weights $\beta_k(\theta)$ satisfy $0 \leq \beta_k(\theta) \leq 1$, $k = 1, \dots, p$ and $\sum_{k=1}^p \beta_k(\theta) = 1$. For this choice of $\beta_k(\theta)$, $p_\theta(i, j)$, $i, j \in S$, $\theta \in \bar{\mathcal{D}}$ can be seen to satisfy the properties of transition probabilities. We now explain the manner in which these weights are obtained. It is worth noting here that the weights $\beta_k(\theta)$ must be continuously differentiable in order to ensure that the extended transition probabilities are continuously differentiable as well and our SASOC algorithms converge. Moreover, in the SASOC algorithms, we do not require an explicit computation of these weights while trying to solve the constrained optimization problem (1). Consider the case when $\theta = \theta_1$ and suppose θ_1 lies between D^j and D^{j+1} (both members of \mathcal{D}). By construction, $\beta_k(\theta_1)$ will correspond to the probability with which projection is done on $[D^j, D^{j+1}]$ and is obtained using the Γ -projection operator as follows: Let us consider an interval of length 2ζ around the midpoint of $[D^j, D^{j+1}]$ and denote it as $[\tilde{D}_1, \tilde{D}_2]$, where $\tilde{D}_1 = \frac{D^j + D^{j+1}}{2} - \zeta$ and $\tilde{D}_2 = \frac{D^j + D^{j+1}}{2} + \zeta$. Then, the weights $\beta_k(\theta_1)$ are set in the following manner: $\beta_k(\theta_1) = 0, \forall k \notin \{j, j+1\}$ and $\beta_j(\theta_1), \beta_{j+1}(\theta_1)$ is given by:

$$(\beta_j(\theta_1), \beta_{j+1}(\theta_1)) = \begin{cases} (1, 0) & \text{if } \theta_1 \in [D^j, \tilde{D}_1] \\ (f(\frac{\tilde{D}_2 - \theta_1}{2\zeta}), 1 - f(\frac{\tilde{D}_2 - \theta_1}{2\zeta})) & \text{if } \theta_1 \in [\tilde{D}_1, \tilde{D}_2] \\ (0, 1) & \text{if } \theta_1 \in [\tilde{D}_2, D^{j+1}] \end{cases} \quad (16)$$

In the above, f to be a continuously differentiable function defined on $[0, 1]$ such that $f(0) = 0$ and $f(1) = 1$ and the Γ -projection is derived from such an f . The above can be similarly extended when the parameter θ

⁵The detailed proofs of the various results are provided in a supplementary file for review

has N components. It can thus be seen that $\beta_k(\theta)$, $k = 1, \dots, p$ are continuously differentiable functions of θ . Thus, from (20) and the fact that $\beta_k(\theta)$ are continuously differentiable, it can be seen that the extended transition dynamics $p_\theta(i, j)$, $\forall \theta \in \bar{\mathcal{D}}, i, j \in S$ are continuously differentiable. We now claim the following:

Lemma 1 *Under the extended dynamics $p_\theta(i, j)$, $i, j \in S$ of the Markov process $\{X_n(\theta)\}$ defined over all $\theta \in \bar{\mathcal{D}}$, we have*

(i) *SASOC-G algorithm is analogous to its continuous counterpart where $\Gamma(\theta)$ and $\Gamma(\theta + \delta\Delta)$ are replaced by $\bar{\Gamma}(\theta)$ and $\bar{\Gamma}(\theta + \delta\Delta)$ respectively.*

(ii) *SASOC-H algorithm is analogous to its continuous counterpart where $\Gamma(\theta)$ and $\Gamma(\theta + \delta_1\Delta + \delta_2\hat{\Delta})$ are replaced by $\bar{\Gamma}(\theta)$ and $\bar{\Gamma}(\theta + \delta_1\Delta + \delta_2\hat{\Delta})$ respectively.*

Step 2: Analysis of fastest timescale recursion

The fastest time-scale in SASOC-G is $\{d(n)\}$ which is used to update the Lagrangian estimates \bar{L} and \bar{L}' corresponding to simulations with θ and $\theta + \delta\Delta$ respectively. First, we show that these estimates indeed converge to the Lagrangian values $L(\theta, \lambda)$ and $L(\theta + \delta\Delta, \lambda)$ defined in (10). By the choice of step-sizes satisfying (A3), we have a time-scale separation between the updates to the Lagrangian estimates \bar{L}_n and the parameters - θ and λ . Hence, for the purpose of analysis of these Lagrangian estimates, θ and λ can be assumed to be time invariant quantities. We now have the following result:

Lemma 2 (i) *For SASOC-G algorithm, $\|\bar{L}(n) - L(\theta(n), \lambda(n))\| \rightarrow 0$ w.p. 1, as $n \rightarrow \infty$.*

(ii) *For SASOC-H algorithm, $\|\bar{L}(n) - L(\theta(n), \lambda(n))\|, \|\bar{L}'(n) - L(\theta(n) + \delta_1\Delta(n) + \delta_2\hat{\Delta}(n), \lambda(n))\| \rightarrow 0$ as $n \rightarrow \infty$.*

Step 3: Analysis of the θ -recursion

We show that the evolution of θ in SASOC-G descends in the Lagrangian value and converges to a limiting set that depends on λ . For this purpose, we first show that the resulting martingale from the θ update recursion in (11) is convergent and then use $V^\lambda(\cdot) = L(\theta, \lambda)$ as an associated Lyapunov function for the following ODE

$$\dot{\theta}(t) = \check{\Gamma}(-\nabla_\theta L(\theta(t), \lambda)), \quad (17)$$

where $\check{\Gamma}$ is defined as follows: For any bounded continuous function $\epsilon(\cdot)$,

$$\check{\Gamma}(\epsilon(\theta(t))) = \lim_{\eta \downarrow 0} \frac{\Gamma(\theta(t) + \eta\epsilon(\theta(t))) - \theta(t)}{\eta}. \quad (18)$$

The projection operator $\check{\Gamma}(\cdot)$ ensures that the evolution of θ via the ODE (23) stays within the bounded set $\bar{\mathcal{D}}$. Again for the analysis of the θ -update, the value of λ which is updated on the slowest time-scale is assumed constant.

Theorem 3 *Under (A1), (A2') and (A3), with $\lambda(n) \equiv \lambda, \forall n$, in the limit as $\delta \rightarrow 0$, $\theta(R) \rightarrow \theta^* \in K^\lambda$ almost surely as $R \rightarrow \infty$, where $K^\lambda = \{\theta \in S : \check{\Gamma}(-\nabla L(\theta(t), \lambda)) = 0\}$.*

Similarly, we show that the parameter updates $\theta(n)$ of SASOC-H converge to a limit point of the ODE

$$\dot{\theta}(t) = \check{\Gamma}(-\Upsilon(\nabla_\theta^2 L(\theta(t), \lambda))^{-1} \nabla_\theta L(\theta(t), \lambda)). \quad (19)$$

Theorem 4 Under (A1), (A2), (A3) and (A4), with $\lambda(n) \equiv \lambda, \forall n$, in the limit as $\delta_1, \delta_2 \rightarrow 0$, $\theta(R) \rightarrow \theta^* \in \bar{K}^\lambda$ almost surely as $R \rightarrow \infty$, where

$$\bar{K}^\lambda = \left\{ \theta \in S : \frac{dL(\theta(t), \lambda)}{dt} = -\nabla_\theta L(\theta(t), \lambda)^T \Upsilon (\nabla_\theta^2 L(\theta(t), \lambda))^{-1} \nabla_\theta L(\theta(t), \lambda) = 0 \right\}.$$

Note that K^λ and \bar{K}^λ can differ in spurious fixed points on the boundary of \bar{D} .

Step 4: : Analysis of the λ -recursion

For $\{\lambda(n)\}$ updates on the slowest time-scale $\{a(n)\}$, we can assume that θ has converged to $\theta^* \in K^\lambda$. We show that $\lambda_{i,j}$ s and λ_f converge respectively to the limit points of the ODEs

$$\begin{aligned} \dot{\lambda}_{i,j}(t) &= \check{\Pi}(G_{i,j}(\theta^*)), \forall i = 1, 2, \dots, |C|, j = 1, 2, \dots, |P|, \\ \dot{\lambda}_f(t) &= \check{\Pi}(H(\theta^*)), \end{aligned}$$

where θ^* is the converged parameter value of SASOC-G/H corresponding to Lagrange parameter $\lambda(t) \triangleq (\lambda_{i,j}(t), \lambda_f(t), i = 1, \dots, |C|, j = 1, \dots, |P|)^T$, and for any bounded continuous functions $\bar{\epsilon}(\cdot)$,

$$\check{\Pi}(\bar{\epsilon}(\lambda(t))) = \lim_{\eta \downarrow 0} \frac{(\lambda(t) + \eta \bar{\epsilon}(\lambda(t)))^+ - \lambda(t)}{\eta}.$$

Here again, the projection operator $\check{\Pi}$ ensures that the evolution of each component of λ stays non-negative. From the definition of the Lagrangian given in (9), the gradient of the Lagrangian w.r.t. $\lambda_{i,j}$ can be seen to be $G_{i,j}(\theta^*)$ and that w.r.t. λ_f is $H(\theta^*)$. Thus, the above ODEs suggest that in SASOC-G/H $\lambda_{i,j}$ s' and λ_f are ascending in the Lagrangian value and converge to a local maximum point. We now have the following result:

Theorem 5 Let $F^{\theta^*} = \{\lambda \geq 0 : \check{\Pi}(G_{i,j}(\theta^*)) = 0, \forall i = 1, 2, \dots, |C|, j = 1, 2, \dots, |P|; \check{\Pi}(H(\theta^*)) = 0\}$. Then, $\lambda(R) \rightarrow \lambda^*$ for some $\lambda^* \in F^{\theta^*}$ w.p. 1 as $R \rightarrow \infty$.

Step 5: Convergence to a locally saddle point

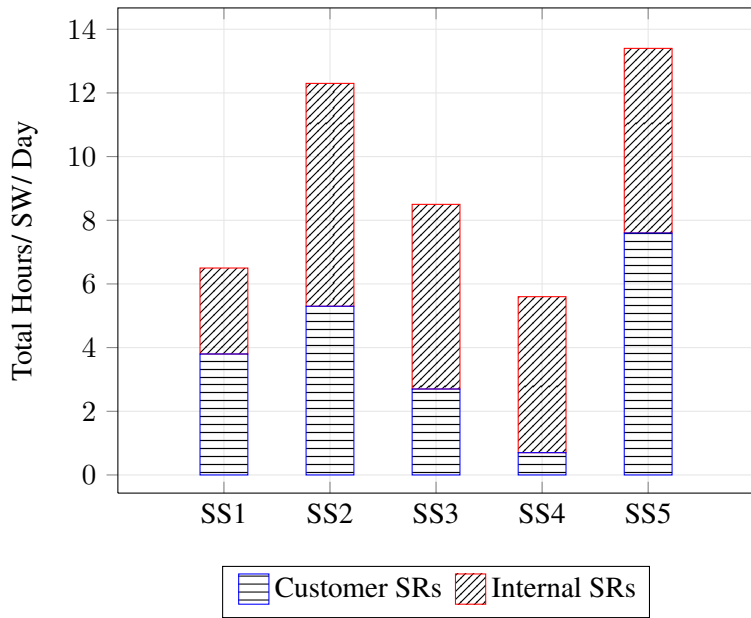
Finally, we argue that the algorithm indeed converges to a (local) saddle point of the Lagrangian. Suppose H_1 denote a local neighborhood in which θ^* is a minimum. Then, through an application of the envelope theorem of mathematical economics (Mas-Colell et al. 1995, pp. 964-966), applied in the ‘Caratheodory sense’ (Borkar 2005, Lemma 4.3, pp.211), it can be seen that

$$\lambda^* \in \arg \min_{\lambda \in H_2} \min_{\theta \in H_1} L(\theta, \lambda),$$

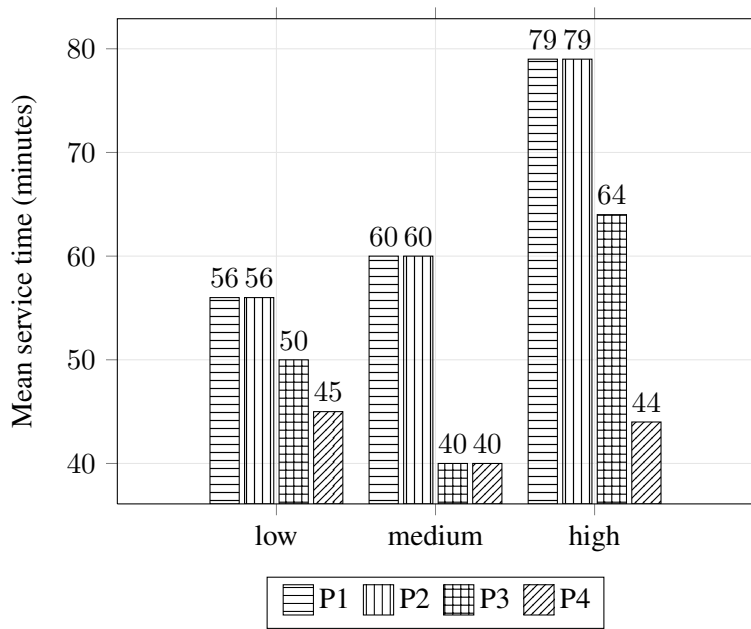
where H_2 is some local neighborhood that contains λ^* . The SASOC algorithms thus converge to a locally saddle point. As mentioned at the beginning of this section, the detailed proofs of the above results are available in an attached supplementary file.

6 Simulation Experiments

We use the simulation framework developed in (Banerjee et al. 2011) for implementing all our algorithms. A number of dispatching policies have been developed in (Banerjee et al. 2011). In particular, we study the PRIO-PULL and EDF policies for performance comparisons of the various algorithms. In addition to the

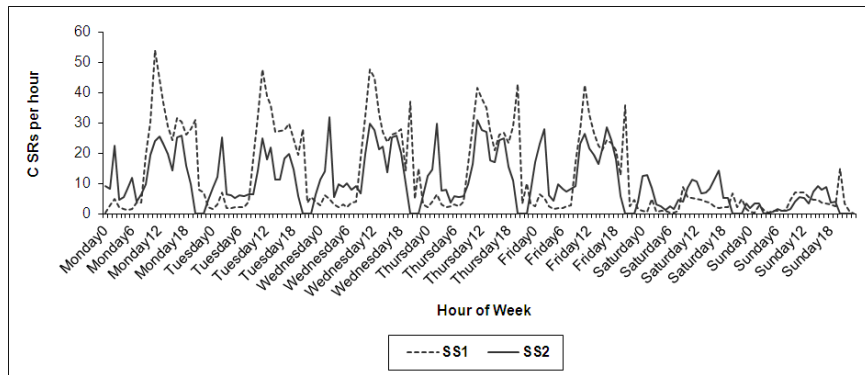


(a) Total work volume statistics for each SS

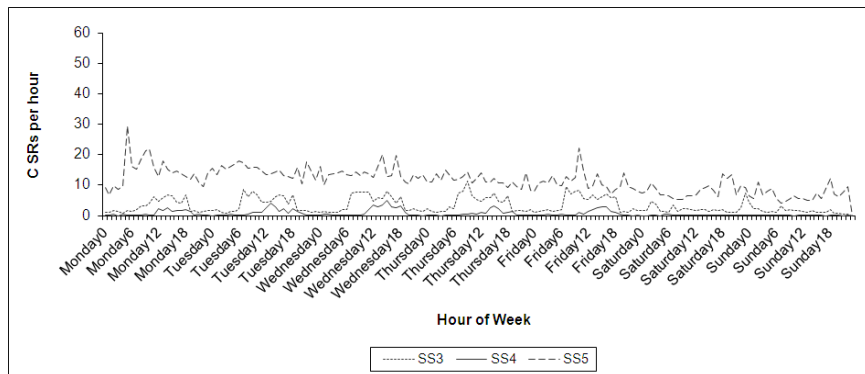


(b) Estimated mean service times for a SS

Figure 4: Characteristics of the service systems used for simulation



(a) SS1 and SS2 work arrival pattern



(b) SS3, SS4 and SS5 work arrival pattern

Figure 5: Work arrival patterns over a week for each SS

three SASOC algorithms, we implemented an algorithm that uses the state-of-the-art optimization tool-kit OptQuest, for the sake of comparison. OptQuest employs an array of techniques including scatter and tabu search, genetic algorithms, and other meta-heuristics for the purpose of optimization and is quite well-known as a hybrid search tool for solving simulation optimization problems ((April et al. 2001)). In particular, we have used the scatter search variant of OptQuest for our experiments.

We choose five real-life SS from two different countries providing server support to IBM’s customers. The five SS cover a variety of characteristics such as high vs. low workload, small vs. large number of customers to be supported, small vs. big staffing levels, and stringent vs. lenient SLA constraints. Collectively, these five SS staff more than 200 SWs with 40%, 30%, and 30% of them having low, medium, and high skill level, respectively. Also, these SS support more than 30 customers each, who make more than 6500 SRs every week with each customer having a distinct pattern of arrival depending on its business hours and seasonality of business domain. Figure 4(a) shows the total work hours per SW per day for each of the SS. The bottom part of the bars denotes customer SR work, i.e., the SRs raised by the customers whereas the top part of the bars denotes internal SR work, i.e, the SRs raised internally for overhead work such as meetings, report generation, and HR activities. This segregation is important because the SLAs apply only to customer SRs. Internal SRs do not have deadlines but they may contribute to queue growth. Note that while average work volumes are significant, they may not directly correlate to SLA attainment. Figure 4(b) shows the effort data, i.e., the mean time taken to resolve an SR (a lognormal distributed random variable in our setting) across priority and complexity classes. As shown in Figures 5, the arrival rates for SS4 and SS5 show much higher peaks than SS1, SS2, and SS3, respectively, although their average work volumes are comparable. The variations are significant because during the peak periods, many SRs may miss their SLA deadlines and influence the optimal staffing result.

Some of the specific details of the service system setting (see Section 3) are as follows: \mathcal{I} , the set of time intervals, contains one element for each hour of the week. Hence, $|\mathcal{I}| = 168$. The set of priority levels, $P = \{P_1, P_2, P_3, P_4\}$, where, $P_1 > P_2 > P_3 > P_4$. The set of skill levels \mathcal{B} is {High, Medium, Low}, where, High > Medium > Low. The simulation framework also involves the swing and preemption policies and the reader is referred to (Banerjee et al. 2011) for a detailed description of this.

We implemented our SASOC algorithms on the simulation framework from (Banerjee et al. 2011) for both the perturbed and the unperturbed simulations (see X and \hat{X} computations in Algorithm 1). For our SASOC algorithms, the simulations were conducted for 1000 iterations, with each iteration having 20 simulation replications - ten each with unperturbed parameter θ and perturbed parameter $\hat{\theta}$, respectively. Each replication simulated the operations of the respective SS for a 30 day period. Thus, we set $R = 1000$ and $K = 10$ for SASOC algorithms. On the other hand, for the OptQuest algorithm, simulations were conducted for 5000 iterations, with each iteration of 100 replications of the SS.

For all the SASOC algorithms, we set the weights in the single-stage cost function $c(X_m)$, see (3), as $r = s = 0.5$. We thus give equal weightage to both the worker utilization and the SLA over-achievement components. The indicator variable q used in the constraint (5) was set to 0 (i.e., infeasible) if the queues were found to grow by 1000% over a two-week period during simulation. We performed a sensitivity study for the paramter δ and found that the choice of 0.5 gave the best results. For the second order methods, the perturbation control parameters δ_1 and δ_2 were both set to 0.5. The function f in the generalized projection operator was set as $f(x) = x$, with the parameter $\zeta = 0.1$. Each of the experiments were run on a machine with dual core Intel 2.1 GHz processor and 3 GB RAM.

The Υ operator implemented for SASOC-W can be described as follows. Let \hat{H} be the Hessian update which needs to be projected. The following sequence of operations represent this projection. (i) $\hat{H} \leftarrow \frac{(\hat{H} + \hat{H}^T)}{2}$; (ii) Perform eigen-decomposition on \hat{H} to get all eigen-values and corresponding eigen-vectors; (iii) Project each eigen-value to $[\epsilon, \frac{1}{\epsilon}]$ where $1 > \epsilon > 0$. ϵ is chosen to be a small number so as to allow for larger range of values, but not too small to avoid singularity. The upper limit in the projection range is to

avoid singularity of the inverse of the Hessian estimate; and (iv) Reconstruct \hat{H} using the projected eigenvalues but with same eigen-vectors. The Υ operator in the case of SASOC-H with diagonal Hessian is one that simply projects each diagonal entry to $[\epsilon, \frac{1}{\epsilon}]$. It is easy to see that the Υ operator satisfies assumption (A4). For a closely related modification of the Hessian, the reader is referred to (Gill et al. 1981). In our experiments, we set $\epsilon = 0.01$.

On each SS, we compare our SASOC algorithms with the OptQuest algorithm using W_{sum} and mean utilization as the performance metrics. Here $W_{sum} \triangleq \sum_{i=1}^{|A|} \sum_{j=1}^{|B|} \theta_{i,j}$ is the sum of workers across shifts and skill levels. The mean utilization here refers to a weighted average of the utilization percentage achieved for each skill level, with the weights being the fraction of the workload corresponding to each skill level.

As evident in Figures 5(a) and 5(b), the SS pools SS1, SS2 and SS3 are characterized by a flat SR arrival pattern, whereas SS4 and SS5 are characterized by a bursty SR arrival pattern. We present and analyze the results on these pools separately, starting with the flat arrival pools in the next section.

6.1 Flat-Arrival SS pools

Figures 6(a) and 6(b) compare the W_{sum}^* achieved for OptQuest and SASOC algorithms using PRIO-PULL and EDF on three real life SS with a flat SR arrival pattern (see Figure 5(a)). Here W_{sum}^* denotes the value obtained upon convergence of W_{sum} . On these SS pools, namely SS1, SS2 and SS3, respectively, we observe that our SASOC algorithms find a better value of W_{sum}^* as compared to OptQuest. Note in particular that on SS1, SASOC algorithms perform significantly better than OptQuest with an improvement of nearly 100%. Further, on SS2, OptQuest is seen to be infeasible whereas all the SASOC algorithms obtain a feasible and good allocation.

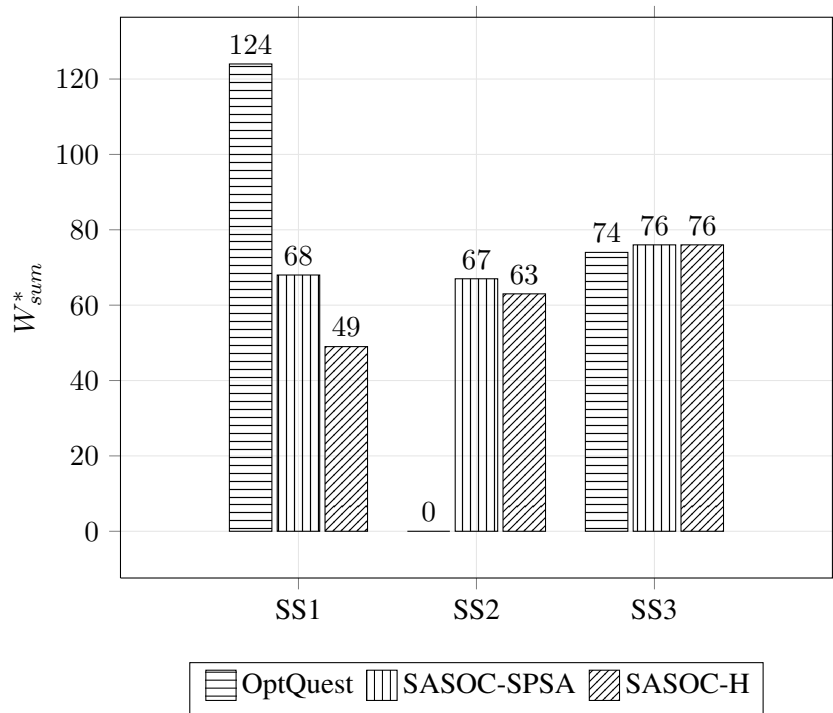
It is evident that SASOC algorithms consistently outperform the OptQuest algorithm on these SS pools. Further, among the SASOC algorithms, we observe that SASOC-W finds better solutions in general as compared to the other two SASOC algorithms. Further, we observe that in all our experiments that include both flat as well as bursty arrival pools, the optimal worker parameter obtained by all our SASOC algorithms is feasible, i.e., satisfies both the SLA as well as the queue stability constraints.

Figure 6(b) presents similar results for the case of the EDF dispatching policy. The behavior of OptQuest and SASOC algorithms was found to be similar to that of PRIO-PULL with SASOC showing performance improvements over OptQuest here as well.

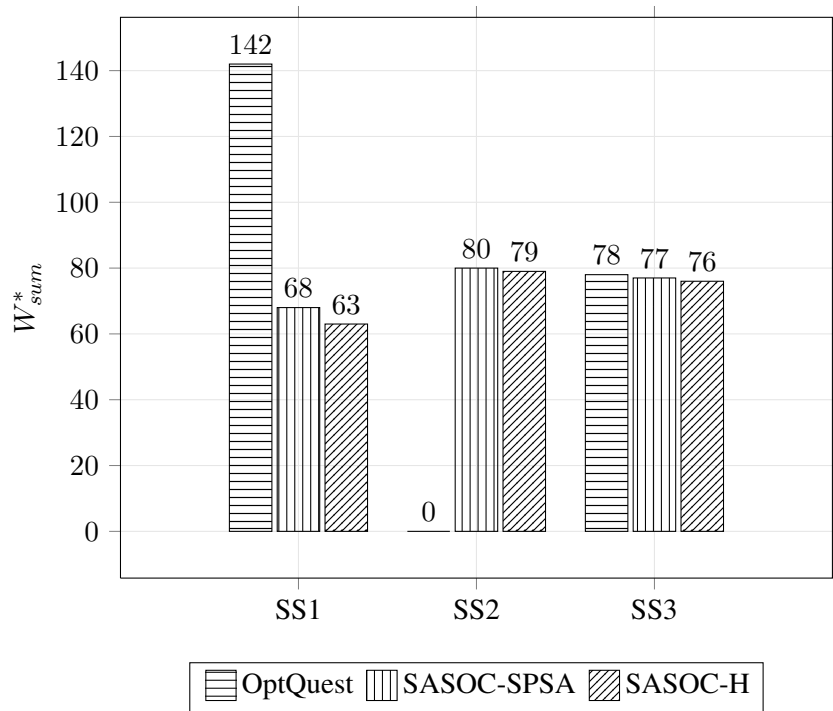
6.2 Bursty-Arrival SS pools

Figures 7(a) and 7(b) compare the W_{sum}^* achieved for OptQuest and SASOC algorithms using PRIO-PULL and EDF on two real life SS with a bursty SR arrival pattern (see Figure 5(b)). From these performance plots, we observe that OptQuest is seen to be slightly better than SASOC-G and SASOC-W when the underlying dispatching policy is PRIO-PULL, whereas in the case of EDF dispatching policy, the SASOC algorithms clearly outperform OptQuest. The execution time advantage of SASOC algorithms over OptQuest hold in the case of these pools as well.

Computational efficiency is a significant factor for any adaptive labor staffing algorithm. For instance, if a candidate labor staffing algorithm takes too long to find the optimal staffing levels, it is not amenable for making staffing changes in a real SS. Both from the number of simulations required as well as the wall clock run time standpoints, SASOC algorithms are better than OptQuest. This is because OptQuest requires 5000 iterations with each iteration of 100 replications, whereas the SASOC algorithms require 1000 iterations of 20 replications each in order to find W_{sum}^* . This results in a 25X speedup for SASOC algorithms and also manifests in the wall clock runtimes of SASOC algorithms because simulation run-times are proportional to the number of SS simulations. We observe that the SASOC algorithms result in at least 10 to 15 times improvement as compared to OptQuest from the wall clock runtimes perspective. For instance, on SS1 the



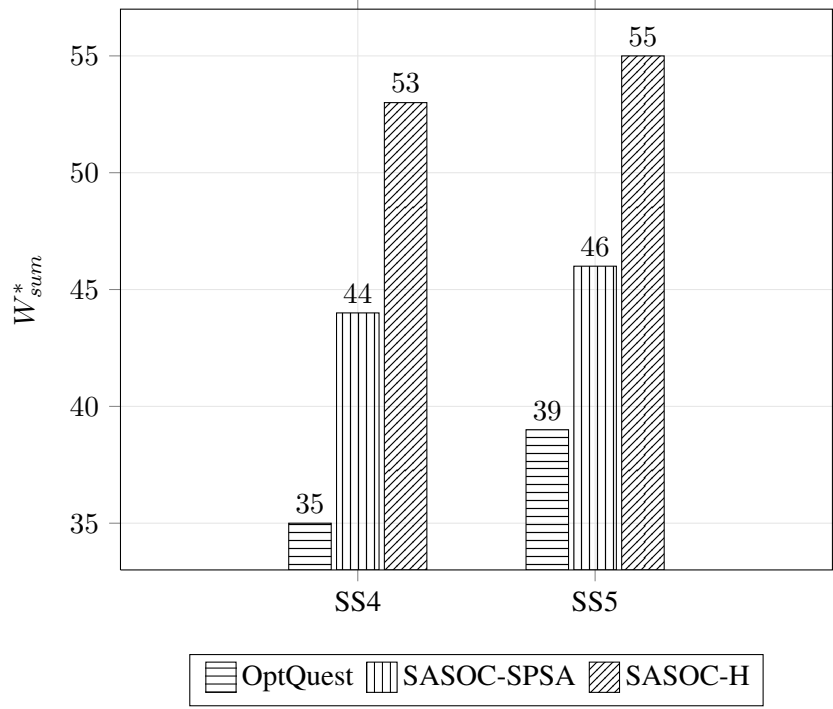
(a) W_{sum}^* for PRIO-PULL



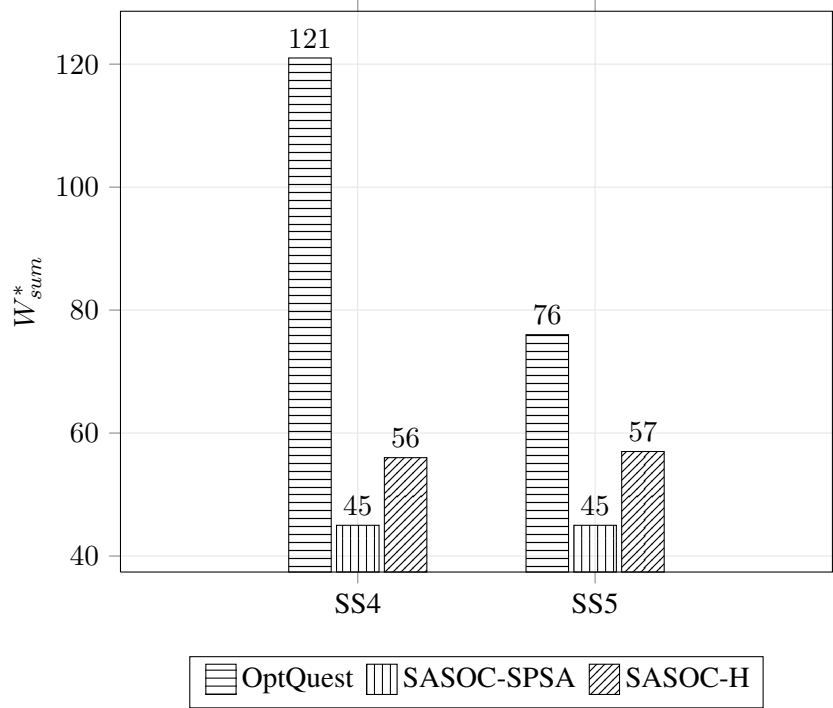
(b) W_{sum}^* for EDF

Figure 6: Performance of OptQuest and SASOC algorithms on SS1, SS2 and SS3^a

^aNote: OptQuest is infeasible over SS2



(a) W_{sum}^* for PRIO-PULL



(b) W_{sum}^* for EDF

Figure 7: Performance of OptQuest and SASOC for two different dispatching policies on SS4 and SS5

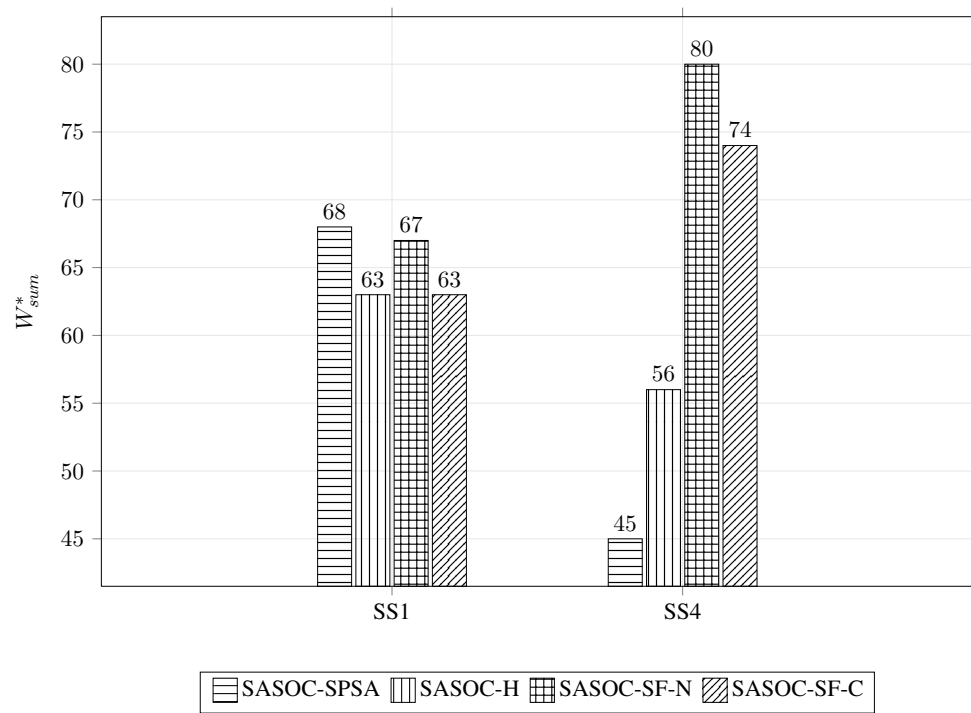


Figure 8: Performance comparison of SASOC with smoothed functional algorithms. ^a

^aNote: the underlying dispatching policy is EDF.

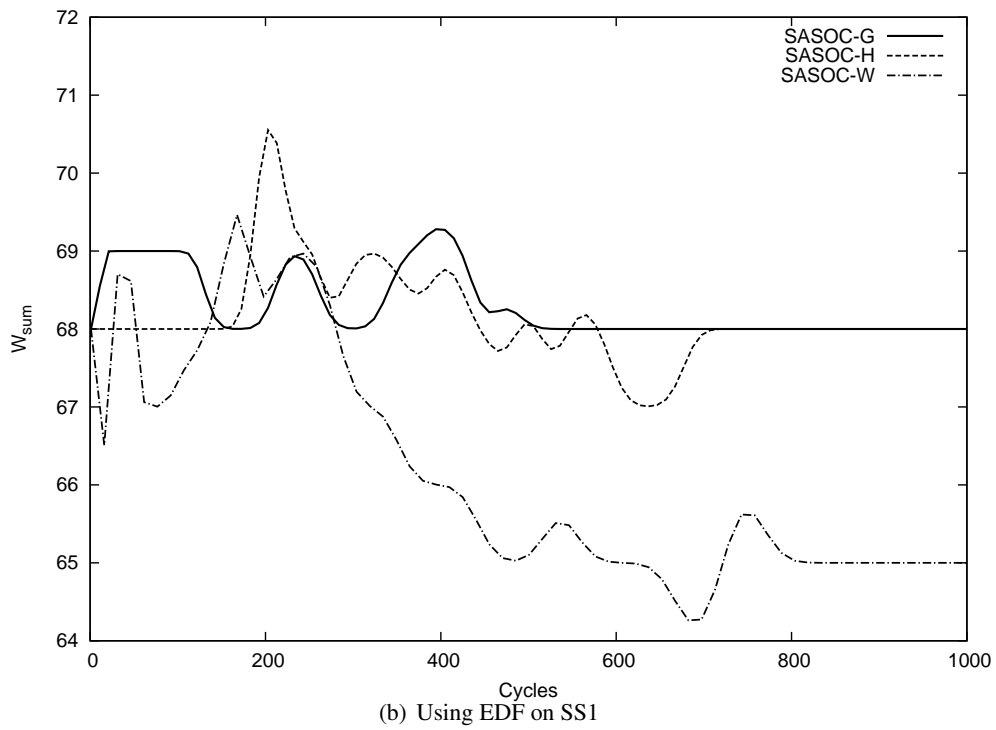
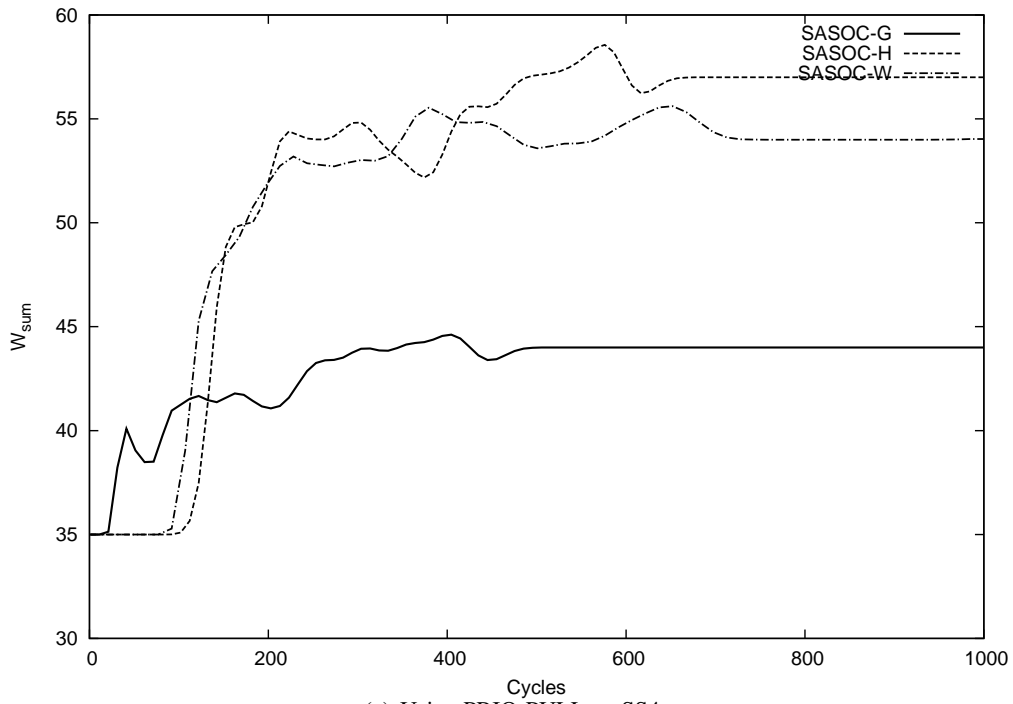


Figure 9: Convergence of W_{sum} as a function of number of cycles for different SASOC algorithms - Illustration on SS1 and SS4 for two dispatching policies

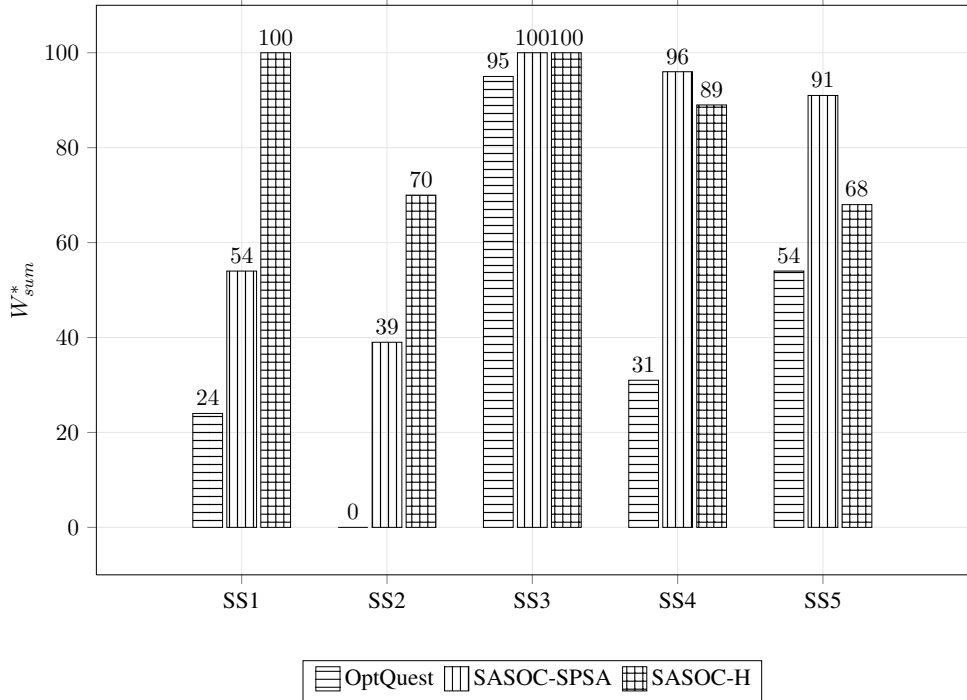


Figure 10: Performance of OptQuest and SASOC for EDF dispatching policy. The mean utilization values have been rounded to nearest integer.

typical run-time of OptQuest was found to be 24 hours, whereas SASOC algorithms took less than 2.5 hours each to converge.

In fact, we observed in the case of SS2, OptQuest does not find a feasible solution even after repeated runs for 5000 search iterations. Also, because OptQuest depends heavily on SLA attainments and respective confidence intervals of previous iterations, it requires higher number of replications than SASOC. Further, we observed that SASOC algorithms converge within 500 iterations in all our experiments. Thus, SASOC algorithms require 25 times less number of simulations as compared to OptQuest, while searching for the optimal SS configuration. This runtime advantage ensures that an SS manager can make staffing changes even at the granularity of every week by making use of SASOC algorithms and the same may not be possible with OptQuest due to its longer runtimes.

6.3 Comparison with SF approaches

Figure 6.1 compares the W_{sum}^* achieved with EDF as the dispatching policy for the SASOC algorithms with the smoothed functional (SF) based schemes from (Prasad et al. 2013). We observe that the SASOC algorithms perform on par with the Cauchy variant (SASOC-SF-C), while performing better than the Gaussian variant of the algorithm from (Prasad et al. 2013). An important advantage with our SASOC algorithms in comparison with the SF based approaches, especially the Cauchy variant, is the low computational overhead. While our algorithms require Bernoulli random variable for perturbing the worker parameter, the SF approaches require Gaussian or Cauchy random variables for the same. Further, the second order method that we propose here (SASOC-H) is more robust in comparison to the first order SF approaches and through the use of Woodbury’s identity, we also achieve low computational overhead as well.

6.4 Empirical Convergence of θ

We observe that the parameter θ (and hence W_{sum}) converges to the optimum value for each of the SS pools considered. This is illustrated by the convergence plots in Figures 9(a) and 9(b). This is a significant feature of SASOC as our algorithms are seen to converge analytically (see Section 5) and the plots confirm the same. In contrast, the OptQuest algorithm is not proven to converge to the optimum even after repeated runs, as illustrated in the case of SS2 in Figure 6(a).

6.5 Mean utilization results

We present the utilization percentages across different skill levels (low, medium and high) in Figure 6.1. The underlying dispatching policy here is EDF. The results for the case of PRIO-PULL are similar. We observe mean utilization of workers is a crucial factor for a labor staffing algorithm and it is evident from Figure 6.1 that SASOC algorithms exhibit a higher mean utilization of workers and hence, better overall performance in comparison to the OptQuest algorithm.

From the above performance comparisons over SS pools with flat as well as bursty SR arrival patterns, it is evident that our SASOC algorithms, which converge to a local saddle point, show overall better performance in comparison with the scatter search-based algorithm of OptQuest. Among the SASOC algorithms, we observe that the second order algorithms (SASOC-H and SASOC-W) perform better than the first order algorithm (SASOC-G) in many cases, with SASOC-W being marginally better than SASOC-H.

7 Conclusions

We motivated the discrete optimization problem of adaptively determining optimal staffing levels in SS and proposed two novel SASOC algorithms for solving this problem. The aim was to find an optimum worker parameter that minimizes a certain long-run cost objective, while adhering to a set of constraint functions, which are also long run averages. All SASOC algorithms are simulation-based optimization methods as the single-stage cost and constraint functions are observable only via simulation and no closed form expressions are available. For solving the constrained optimization problem, we applied the Lagrange relaxation procedure and used an SPSA based scheme for performing gradient descent in the primal and at the same time, ascent in the dual, for the Lagrange multipliers. All SASOC algorithms also incorporated a smooth (generalized) projection operator that helped imitate a continuous parameter system with suitably defined transition dynamics. Using the theory of multi-timescale stochastic approximation, we presented the convergence proof of our algorithms. Numerical experiments were performed to evaluate each of the algorithms based on real-life SS data against the state-of-the-art simulation optimization toolkit OptQuest in the current context. SASOC algorithms in general showed overall superior performance compared to OptQuest, as they (a) exhibited more than an order of magnitude faster convergence than OptQuest, (b) consistently found solutions of good quality and in most cases better than those found by OptQuest, and (c) showed guaranteed convergence even in scenarios where OptQuest did not find feasibility even after repeated runs for 5000 iterations. Given the quick convergence of SASOC algorithms (in minutes), they are particularly suitable for adaptive labor staffing where a few days of optimization run like in OptQuest would fail to keep up with the changes. By comparing the results of the SASOC algorithms on two independent dispatching policies, we showed that SASOC's performance is independent of the operational model of SS.

As future work, one may consider single-stage cost function enhancements that include worker salaries as well as other relevant monetary costs, apart from staff utilization and SLA attainment factors. An orthogonal direction of future work in this context is to develop skill updation algorithms, i.e., derive novel work dispatch policies that improve the skills of the workers beyond their current levels by way of assigning work of a higher complexity. However, the setting is still constrained and the SLAs would need to be met

while improving the skill levels of the workers. The skill updation scheme could then be combined with the SASOC algorithms presented in this paper to optimize the staffing levels on a slower timescale.

A Appendix: Convergence Analysis

Here we provide a sketch of the convergence of the SASOC-G and SASOC-H algorithms. The first step in the convergence analysis is common to all the SASOC algorithms and involves the extension of the transition dynamics $p_\theta(i, j)$ of the constrained parameterized hidden Markov process to the convex hull $\bar{\mathcal{D}}$.

Extension of the transition dynamics $p_{i,j}(\theta)$

Recall that the discrete parameter θ of the Markov process $\{X_n(\theta)\}$ takes values in the set \mathcal{D} defined earlier. Using the members of \mathcal{D} , one can extend the transition dynamics $p_\theta(i, j)$ of the underlying Markov process to any θ in the convex hull $\bar{\mathcal{D}}$ as follows:

$$p_\theta(i, j) = \sum_{k=1}^p \beta_k(\theta) p_{D^k}(i, j), \quad \forall \theta \in \bar{\mathcal{D}}, i, j \in S, \quad (20)$$

where the weights $\beta_k(\theta)$ satisfy $0 \leq \beta_k(\theta) \leq 1, k = 1, \dots, p$ and $\sum_{k=1}^p \beta_k(\theta) = 1$. $p_\theta(i, j), i, j \in S, \theta \in \bar{\mathcal{D}}$ can be seen to satisfy the properties of transition probabilities. It is worth noting here that the weights $\beta_k(\theta)$ must be continuously differentiable in order to ensure that the extended transition probabilities are continuously differentiable as well and our SASOC algorithms converge. Moreover, in the SASOC algorithms, we do not require an explicit computation of these weights while trying to solve the constrained optimization problem equation (1) of the main paper. Consider the case when $\theta = (\theta_1)^T$ and suppose θ_1 lies between D^j and D^{j+1} (both members of \mathcal{D}). By construction, $\beta_k(\theta)$ will correspond to the probability with which projection is done on $[D^j, D^{j+1}]$ and is obtained using the Γ -projection operator as follows: Let us consider an interval of length 2ζ around the midpoint of $[D^j, D^{j+1}]$ and denote it as $[\tilde{D}_1, \tilde{D}_2]$, where $\tilde{D}_1 = \frac{D^j + D^{j+1}}{2} - \zeta$ and $\tilde{D}_2 = \frac{D^j + D^{j+1}}{2} + \zeta$. Then, the weights $\beta_k(\theta)$ are set in the following manner: $\beta_k(\theta) = 0, \forall k \notin \{j, j+1\}$ and $\beta_j(\theta), \beta_{j+1}(\theta)$ is given by:

$$(\beta_j(\theta_1), \beta_{j+1}(\theta_1)) = \begin{cases} (1, 0) & \text{if } \theta \in [D^j, \tilde{D}_1] \\ (f(\frac{\tilde{D}_2 - \theta_1}{2\zeta}), 1 - f(\frac{\tilde{D}_2 - \theta_1}{2\zeta})) & \text{if } \theta_1 \in [\tilde{D}_1, \tilde{D}_2] \\ (0, 1) & \text{if } \theta \in [\tilde{D}_2, D^{j+1}] \end{cases} \quad (21)$$

In the above, f is obtained from the definition of Γ -projection and hence, is a continuously differentiable function defined on $[0, 1]$ such that $f(0) = 0$ and $f(1) = 1$. The above can be similarly extended when the parameter θ has N components. It can thus be seen that $\beta_k(\theta), k = 1, \dots, p$ are continuously differentiable functions of θ . Thus, from (20) and the fact that $\beta_k(\theta)$ are continuously differentiable, it can be seen that the extended transition dynamics $p_\theta(i, j), \forall \theta \in \bar{\mathcal{D}}, i, j \in S$ are continuously differentiable.

We now claim the following:

Lemma 6 For any $\theta \in \bar{\mathcal{D}}, \{X_n(\theta), n \geq 0\}$ is ergodic Markov.

Proof: Follows in a similar manner as Lemma 2 of Bhatnagar et al. (2011b). ■

Now, define analogues of the long-run average cost and constraint functions for any $\theta \in \bar{\mathcal{D}}$ as follows:

$$\begin{aligned}
\bar{J}(\theta) &\triangleq \lim_{n \rightarrow \infty} \frac{1}{n} \sum_{m=0}^{n-1} c(X_m(\theta)), \theta \in \bar{\mathcal{D}} \\
\bar{G}_{i,j}(\theta) &\triangleq \lim_{n \rightarrow \infty} \frac{1}{n} \sum_{m=0}^{n-1} g_{i,j}(X_m(\theta)) \leq 0, \\
&\quad \forall i = 1, \dots, |C|, j = 1, \dots, |P|, \theta \in \bar{\mathcal{D}} \\
\bar{H}(\theta) &\triangleq \lim_{n \rightarrow \infty} \frac{1}{n} \sum_{m=0}^{n-1} h(X_m(\theta)) \leq 0, \theta \in \bar{\mathcal{D}}.
\end{aligned} \tag{22}$$

The difference between the above and the corresponding entities defined in equation (1) of the main paper is that θ can take values in $\bar{\mathcal{D}}$ in the above. In lieu of Lemma 2, the above limits are well-defined for all $\theta \in \bar{\mathcal{D}}$.

Lemma 7 $\bar{J}(\theta), \bar{G}_{i,j}(\theta), i = 1, \dots, |C|, j = 1, \dots, |P|$, and $\bar{H}(\theta)$ are continuously differentiable in $\theta \in \bar{\mathcal{D}}$.

Proof: Follows in a similar manner as Lemma 3 of Bhatnagar et al. (2011b). ■

We now prove the SASOC algorithms described previously are equivalent to their analogous continuous parameter $\bar{\theta}$ counterparts under the extended Markov process dynamics.

Lemma 8 Under the extended dynamics $p_{\theta}(i, j), i, j \in S$ of the Markov process $\{X_n(\theta)\}$ defined over all $\theta \in \bar{\mathcal{D}}$, we have

- (i) SASOC-G algorithm is analogous to its continuous counterpart where $\Gamma(\theta)$ and $\Gamma(\theta + \delta\Delta)$ are replaced by $\bar{\Gamma}(\theta)$ and $\bar{\Gamma}(\theta + \delta\Delta)$ respectively.
- (ii) SASOC-H algorithm is analogous to its continuous counterparts where $\Gamma(\theta)$ and $\Gamma(\theta + \delta_1\Delta + \delta_2\hat{\Delta})$ are replaced by $\bar{\Gamma}(\theta)$ and $\bar{\Gamma}(\theta + \delta_1\Delta + \delta_2\hat{\Delta})$ respectively.

Proof: (i): Consider the SASOC-G algorithm which updates according to equation (11) of the main paper. Let $\theta(m)$ be a given parameter update that lies in $\bar{\mathcal{D}}^\circ$ (where $\bar{\mathcal{D}}^\circ$ denotes the interior of the set $\bar{\mathcal{D}}$). Let $\delta > 0$ be sufficiently small so that $\bar{\theta}^1(m) = (\bar{\Gamma}_j(\theta_j(m) + \delta\Delta_j(m)), j = 1, \dots, N)^T = (\theta_j(m) + \delta\Delta_j(m)), j = 1, \dots, N)^T$.

Consider now the Γ -projected parameters $\theta^1(m) = (\Gamma_j(\theta_j(m) + \delta\Delta_j(m)), j = 1, \dots, N)^T$ and $\theta^2(m) = (\Gamma_j(\theta_j(m)), j = 1, \dots, N)^T$, respectively. By the construction of the generalized projection operator, these parameters are equal to $\theta^k \in C$ with probabilities $\beta_k((\theta_j(m) + \delta\Delta_j(m)), j = 1, \dots, N)^T$ and $\beta_k(\theta_j(m), j = 1, \dots, N)^T$, respectively. When the operative parameter is θ^k , the transition probabilities are $p_{\theta^k}(i, l), i, l \in S$. Thus with probabilities $\beta_k((\theta_j(m) + \delta\Delta_j(m)), j = 1, \dots, N)^T$ and $\beta_k(\theta_j(m), j = 1, \dots, N)^T$, respectively, the transition probabilities in the two simulations equal $p_{\theta^k}(i, l), i, l \in S$.

Next, consider the alternative (extended) system with parameters $\bar{\theta}^1(m) = (\bar{\Gamma}_j(\theta_j(m) + \delta\Delta_j(m))$ and $\bar{\theta}^2(m) = \bar{\Gamma}_j(\theta_j(m))$, respectively. The transition probabilities are now given by

$$p_{\bar{\theta}^i(m)}(j, l) = \sum_{k=1}^p \beta_k(\bar{\theta}^i(m)) p_{\theta^k}(j, l),$$

$i = 1, 2, j, l \in S$. Thus with probability $\beta_k(\bar{\theta}^i(m))$, a transition probability of $p_{\theta^k}(j, l)$ is obtained in the i th system. Thus the two systems (original and the one with extended dynamics) are analogous.

Now consider the case when $\theta(m) \in \partial\bar{D}$, i.e., is a point on the boundary of \bar{D}). Then, one or more components of $\theta(m)$ are extreme points. For simplicity, assume that only one component (say the i th component) is an extreme point as the same argument carries over if there are more parameter components that are extreme points. By the i th component of $\theta(m)$ being an extreme point, we mean that $\theta_i(m)$ is either 0 or W_{\max} . The other components $j = 1, \dots, N, j \neq i$ are not extreme. Thus, $\theta_i(m) + \delta\Delta_i(m)$ can lie outside of the interval $[0, W_{\max}]$. For instance, suppose that $\theta_i(m) = W_{\max}$ and that $\theta_i(m) + \delta\Delta_i(m) > W_{\max}$ (which will happen if $\Delta_i(m) = +1$). In such a case, $\theta_i^1(m) = \Gamma_i(\theta_i(m) + \delta\Delta_i(m)) = W_{\max}$ with probability one. Then, as before, $\theta^1(m)$ can be written as the convex combination $\theta^1(m) = \sum_{k=1}^p \beta_k(\theta^1(m))\theta^k$ and the rest follows as before.

(ii): Follows in a similar manner as part (i) above. ■

As a consequence of Lemma 8, we can analyze the SASOC algorithms with the continuous parameter $\bar{\theta}$ used in place of θ and under the extended transition dynamics (20). By an abuse of notation, we shall henceforth use θ to refer to the latter.

SASOC-G

The convergence analysis of SASOC-G can be split into four stages:

(I) The fastest time-scale in SASOC-G is $\{d(n)\}$ which is used to update the Lagrangian estimates \bar{L} and \bar{L}' corresponding to simulations with θ and $\theta + \delta\Delta$ respectively. Firstly, we show that these estimates indeed converge to the Lagrangian values $L(\theta, \lambda)$ and $L(\theta + \delta\Delta, \lambda)$ defined in equation (9) of the main paper. Note that the θ and λ which are updated on slower time-scales, can be assumed to be time invariant quantities for the purpose of analysis of these Lagrangian estimates.

(II) Next, we show that the parameter updates $\theta(n)$ using SASOC-G converge to a limit point of the ODE

$$\dot{\theta}(t) = \check{\Gamma}(-\nabla_{\theta}L(\theta(t), \lambda)), \quad (23)$$

where $\check{\Gamma}$ is defined as follows: For any bounded continuous function $\epsilon(\cdot)$,

$$\check{\Gamma}(\epsilon(\theta(t))) = \lim_{\eta \downarrow 0} \frac{\Pi(\theta(t) + \eta\epsilon(\theta(t))) - \theta(t)}{\eta}. \quad (24)$$

The projection operator $\check{\Gamma}(\cdot)$ ensures that the evolution of θ stays within the bounded set M . Again for the analysis of the θ -update, the value of λ which is updated on the slowest time-scale is assumed constant.

(III) We show that $\lambda_{i,j}s$ and λ_f converge respectively to the limit points of the ODEs

$$\begin{aligned} \dot{\lambda}_{i,j}(t) &= \check{\Pi}(G_{i,j}(\theta^*)), \forall i = 1, 2, \dots, |C|, j = 1, 2, \dots, |P|, \\ \dot{\lambda}_f(t) &= \check{\Pi}(H(\theta^*)), \end{aligned}$$

where θ^* is the converged parameter value of SASOC-G/H corresponding to Lagrange parameter $\lambda(t) \triangleq (\lambda_{i,j}(t), \lambda_f(t), i = 1, \dots, |C|, j = 1, \dots, |P|)^T$, and for any bounded continuous functions $\bar{\epsilon}(\cdot)$,

$$\check{\Pi}(\bar{\epsilon}(\lambda(t))) = \lim_{\eta \downarrow 0} \frac{(\lambda(t) + \eta\bar{\epsilon}(\lambda(t)))^+ - \lambda(t)}{\eta}.$$

Here again, the projection operator $\check{\Pi}$ ensures that the evolution of each component of λ stays non-negative. From the definition of the Lagrangian given in equation (9) of the main paper, the gradient of the Lagrangian w.r.t. $\lambda_{i,j}$ can be seen to be $G_{i,j}(\theta^*)$ and that w.r.t. λ_f to be $H(\theta^*)$. Thus, the above ODEs suggest that in SASOC-G $\lambda_{i,j}s$ and λ_f are ascending in the Lagrangian value and converge to a local maximum point.

(IV) Finally, we show that the algorithm indeed converges to a (local) saddle point of the Lagrangian with local maximum in $\lambda_{i,j}s$ and λ_f , and local minimum in θ .

Lemma 9 $\|\bar{L}(n) - L(\theta(n), \lambda(n))\| \rightarrow 0$ w.p. 1, as $n \rightarrow \infty$.

Proof: θ and λ values are being updated on slower time-scales, thus assumed to be constant in this proof.

Let

$$l(X_m) \triangleq c(X_{nK+m}) + \sum_{i=1}^{|C|} \sum_{j=1}^{|P|} \lambda_{i,j}(nK) g_{i,j}(X_{nK+m}) + \lambda_f h(X_{nK+m}).$$

The \bar{L} update can be re-written as

$$\bar{L}(m+1) = \bar{L}(m) + d(m) (L(\theta(m), \lambda(m)) + \xi_1(m) - \bar{L}(m) + M_{m+1}),$$

where $\xi_1(m) = (E[l(X_m)|\mathcal{F}_{m-1}] - L(\theta(m), \lambda(m)))$, $m \geq 0$ and

$\mathcal{F}_m = \sigma(X_n, \lambda(n), \theta(n), n \leq m)$, $m \geq 0$ are the associated σ -fields. Also, $M_{m+1} = l(X_m) - E[l(X_m)|\mathcal{F}_{m-1}]$, $m \geq 0$ is a martingale difference sequence. Let $N_m = \sum_{n=0}^m d(n)M_{n+1}$. It can be easily verified that (N_m, \mathcal{F}_m) , $m \geq 0$ is a square-integrable martingale obtained from the corresponding martingale difference $\{M_m\}$. Further, from the square summability of $d(n)$, $n \geq 0$, and the facts that S is compact and l is Lipschitz continuous, it can be verified from the martingale convergence theorem that $\{N_m, m \geq 0\}$, converges almost surely.

Now from Lemma 6 $\{(X_m)\}$ is ergodic Markov for any given $\theta(m)$. Hence, $|E[l(X_m)|\mathcal{F}_{m-1}] - L(\theta(m), \lambda(m))| \rightarrow 0$ almost surely on the ‘natural timescale’, as $m \rightarrow \infty$. The ‘natural timescale’ is clearly faster than the algorithm’s timescale and hence $\xi_1(m)$ can be ignored in the analysis of \bar{L} -recursion, see (Borkar 2008, Chapter 6.2) for detailed treatment of natural timescale algorithms. The rest of the proof follows from the Hirsch lemma (Hirsch 1989, Theorem 1, pp. 339). ■

On similar lines, $\|\bar{L}'(n) - L(\theta(n) + \delta\Delta(n), \lambda(n))\| \rightarrow 0$ w.p. 1, as $n \rightarrow \infty$. Thus, θ updates which are on the slower time scale $\{b(n)\}$, can be re-written as

$$W_i(n+1) = W_i(n) - b(n) \left(\frac{L(\theta(n) + \delta\Delta_i(n), \lambda) - L(\theta(n), \lambda)}{\delta\Delta_i(n)} \right) + b(n)\chi_{n+1}, \quad (25)$$

$\forall i = 1, 2, \dots, |A| \times |B|$, where $\chi_n = o(1)$ in view of Lemma 9. Note here that $\lambda(n) \equiv \lambda$, $\forall n$. Now for the ODE (23), $V^\lambda(\cdot) = L(\cdot, \lambda)$ serves as an associated Lyapunov function and the stable fixed points of this ODE lie within the set $K^\lambda = \{\theta \in S : \check{\Gamma}(-\nabla L(\theta(t), \lambda)) = 0\}$.

Theorem 10 Under (A1)-(A3), in the limit as $\delta \rightarrow 0$, $\theta(R) \rightarrow \theta^* \in K^\lambda$ almost surely as $R \rightarrow \infty$. *Proof:* From assumption (A2), $L(\theta, \lambda)$ is assumed to be continuous. Hence over the compact set M , $L(\theta, \lambda)$ is uniformly bounded. Thus, from Lasalle’s invariance theorem Lasalle and Le fschetz (1961) (Kushner and Yin 1997, Theorem 2.3, pp. 76), $\theta(R) \rightarrow \theta^* \in K^\lambda$ a.s. as $R \rightarrow \infty$. ■

Thus (25) can be seen to be an Euler discretization of (23) and converges a.s. to K^λ in the limit as $\delta \rightarrow 0$.

For $\{\lambda(n)\}$ updates on the slowest time-scale $\{a(n)\}$, we can assume that θ has converged to $\theta^* \in K^\lambda$. Let

$$F^{\theta^*} = \{\lambda \geq 0 : \check{\Pi}(G_{i,j}(\theta^*)) = 0, \forall i = 1, 2, \dots, |C|, j = 1, 2, \dots, |P|; \check{\Pi}(H(\theta^*)) = 0\}.$$

Theorem 11 $\lambda(R) \rightarrow \lambda^* \in F$ w.p. 1 as $R \rightarrow \infty$. *Proof:* The λ update in equation (11) of the main paper can be re-written as

$$\lambda_{i,j}(n+1) = \lambda_{i,j}(n) + a(n) [G_{i,j}(\theta^*) + N_{n+1} + M_{n+1}],$$

where $N_{n+1} = E[g_{i,j}(X_n)|\mathcal{F}_{n-1}] - G_{i,j}(\theta^*)$, $M_{n+1} = g_{i,j}(X_n) - E[g_{i,j}(X_n)|\mathcal{F}_{n-1}]$. It is easy to see that from Lemma 6 that $N_n \rightarrow 0$ as $n \rightarrow \infty$ along the natural timescale (see Lemma 9). Further, $\{M_n\}$ is a martingale difference sequence with $\sum_{i=0}^n a(i)M_{i+1}$, $n \geq 0$, being the associated martingale that can be seen to be a.s. convergent (See Prop. 4.4 of Bhatnagar et al. (2011a)). Thus from (Borkar 2008, Extension 3 of Section 2.2), the result follows for $\lambda_{i,j}$ s. Similarly, one can show convergence for λ_f . ■

Now, we need to show that the convergence of the algorithm is indeed to a saddle point, i.e., $\theta^* \in K^{\lambda^*}$ and $\lambda^* \in F^{\theta^*}$. This can be shown by invoking the envelope theorem of mathematical economics (Mas-Colell et al. 1995, pp. 964-966); see remark (2) in (Bhatnagar et al. 2011a, pp 15).

SASOC-H

Convergence analysis of SASOC-H follows along similar lines as that of the SASOC-G algorithm as given below. Note that we first analyse the case when the Hessian is inverted directly in SASOC-H and then give the necessary modifications for the proof to work when Woodbury's identity is employed.

1. As in Lemma 9, one can see that \bar{L} and \bar{L}' iterations converge almost surely as follows:

$$\|\bar{L}(n) - L(\theta(n), \lambda(n))\|, \|\bar{L}'(n) - L(\theta(n) + \delta_1 \Delta(n) + \delta_2 \widehat{\Delta}(n), \lambda(n))\| \rightarrow 0 \text{ as } n \rightarrow \infty.$$

2. Next, we show that the parameter updates $\theta(n)$ of SASOC-H converge to a limit point of the ODE

$$\dot{\theta}(t) = \check{\Gamma} \left(-\Upsilon(\nabla_{\theta}^2 L(\theta(t), \lambda))^{-1} \nabla_{\theta} L(\theta(t), \lambda) \right), \quad (26)$$

where $\check{\Gamma}$ is as defined in equation (24).

3. The rest of the analysis of slower time-scale updates of $\lambda_{i,j}$ s and λ_f , and saddle point behaviour follows from that of SASOC-G.

Lemma 12

$$\left\| \frac{L(\theta(n) + \delta_1 \Delta(n) + \delta_2 \widehat{\Delta}(n), \lambda(n)) - L(\theta(n), \lambda(n))}{\delta_2 \widehat{\Delta}_i(n)} - \nabla_{\theta_i} L(\theta(n), \lambda(n)) \right\| \rightarrow 0 \text{ w.p. } 1,$$

with $\delta_1, \delta_2 \rightarrow 0$ as $n \rightarrow \infty \quad \forall i \in \{1, 2, \dots, |A| \times |B|\}$. *Proof:* Follows from (Bhatnagar et al. 2011a, Proposition 4.10). ■

Lemma 13

$$\left\| \frac{L(\theta(n) + \delta_1 \Delta(n) + \delta_2 \widehat{\Delta}(n), \lambda(n)) - L(\theta(n), \lambda(n))}{\delta_1 \Delta_i(n) \delta_2 \widehat{\Delta}_j(n)} - \nabla_{\theta_{i,j}}^2 L(\theta(n), \lambda(n)) \right\| \rightarrow 0 \text{ w.p. } 1,$$

with $\delta_1, \delta_2 \rightarrow 0$ as $n \rightarrow \infty, \quad \forall i, j \in \{1, 2, \dots, |A| \times |B|\}$. *Proof:* Follows from (Bhatnagar et al. 2011a, Proposition 4.9). ■

Lemma 14

$$\left\| H_{i,j}(n) - \nabla_{\theta_{i,j}}^2 L(\theta(n), \lambda(n)) \right\| \rightarrow 0 \text{ w.p. } 1,$$

with $\delta_1, \delta_2 \rightarrow 0$ as $n \rightarrow \infty, \quad \forall i, j \in \{1, 2, \dots, |A| \times |B|\}$.

Proof: Follows from Lemma 13 applied to the Hessian update of SASOC-H. ■

Lemma 15

$$\|M(n) - \Upsilon(\nabla_{\theta}^2 L(\theta(n), \lambda(n)))^{-1}\| \rightarrow 0 \text{ w.p. } 1,$$

with $\delta_1, \delta_2 \rightarrow 0$ as $n \rightarrow \infty$, $\forall i, j \in \{1, 2, \dots, |A| \times |B|\}$.

Proof: Follows from Lemma 14 and (Bhatnagar 2007, Lemma A.9). ■

Let

$$\bar{K}^{\lambda} = \left\{ \theta \in S : \frac{dL(\theta(t), \lambda)}{dt} = -\nabla_{\theta} L(\theta(t), \lambda)^T \Upsilon(\nabla_{\theta}^2 L(\theta(t), \lambda))^{-1} \nabla_{\theta} L(\theta(t), \lambda) = 0 \right\}.$$

Theorem 16 *Under assumptions (A1)-(A4), in the limit as $\delta_1, \delta_2 \rightarrow 0$, $\theta(R) \rightarrow \theta^* \in \bar{K}^{\lambda}$ almost surely as $R \rightarrow \infty$. *Proof:* Following Lemmas 9, 12 and 15, with $\delta_1, \delta_2 \rightarrow 0$, the update of parameter θ can be re-written in vector form as*

$$\theta_{n+1} = \Pi(\theta_n - b(n) \Upsilon(\nabla_{\theta}^2 L(\theta(t), \lambda))^{-1} \nabla_{\theta} L(\theta(t), \lambda) + b(n) \chi_n)$$

with $\chi_n = o(1)$. Thus, the update of parameter θ can be viewed as a noisy Euler discretization of the ODE (26) using a standard approximation argument as in (Kushner and Clark 1978, pp. 191-196). Note that $V^{\lambda}(\cdot) = L(\cdot, \lambda)$ itself serves as the associated Lyapunov function (Kushner and Yin 1997, pp. 75) for the ODE (26) with stable limit points of the ODE lying within the set \bar{K}^{λ} . From assumption (A2), $L(\theta, \lambda)$ is assumed to be continuous. Hence over the compact set M , $L(\theta, \lambda)$ is uniformly bounded. Thus, from Lasalle's invariance theorem Lasalle and Le fschetz (1961), $\theta(n) \rightarrow \theta^* \in K^{\lambda}$ a.s. as $n \rightarrow \infty$. ■

Convergence analysis of SASOC-H when the Hessian is inverted using an iterative procedure based on Woodbury's identity, follows from the above analysis for the SASOC-H algorithm (with direct inversion of the Hessian) given the following lemma instead of Lemma 15.

Lemma 17

$$\|M(n) - \Upsilon(\nabla_{\theta}^2 L(\theta(n), \lambda(n)))^{-1}\| \rightarrow 0 \text{ w.p. } 1,$$

with $\delta_1, \delta_2 \rightarrow 0$ as $n \rightarrow \infty$, $\forall i, j \in \{1, 2, \dots, |A| \times |B|\}$. *Proof:* From Woodbury's identity, since $M(n), n \geq 1$ sequence of SASOC-W is identical to the $\Upsilon(H(n))^{-1}, n \geq 1$ sequence of SASOC-H, the result follows from Lemma 15. ■

References

- S. Alter. Service system fundamentals: Work system, value chain, and life cycle. *IBM Systems Journal*, 47(1):71–85, 2008.
- J. April, F. Glover, J. Kelly, and M. Laguna. Simulation/optimization using "real-world" applications. In *Winter Simulation Conference*, volume 1, pages 134–138, 2001.
- D. Banerjee, N. Desai, and G. Dasgupta. Simulation-based evaluation of dispatching policies in service systems. In *Winter simulation conference*, 2011.
- S. Bhatnagar. Adaptive multivariate three-timescale stochastic approximation algorithms for simulation based optimization. *ACM Transactions on Modeling and Computer Simulation (TOMACS)*, 15(1):74–107, 2005.

- S. Bhatnagar. Adaptive Newton-based multivariate smoothed functional algorithms for simulation optimization. *ACM Transactions on Modeling and Computer Simulation (TOMACS)*, 18(1):1–35, 2007.
- S. Bhatnagar, M.C. Fu, S.I. Marcus, and I. Wang. Two-timescale simultaneous perturbation stochastic approximation using deterministic perturbation sequences. *ACM Transactions on Modeling and Computer Simulation (TOMACS)*, 13(2):180–209, 2003. ISSN 1049-3301.
- S. Bhatnagar, N. Hemachandra, and V.K. Mishra. Stochastic approximation algorithms for constrained optimization via simulation. *ACM Transactions on Modeling and Computer Simulation (TOMACS)*, 21(3):15, 2011a.
- S. Bhatnagar, V. Mishra, and N. Hemachandra. Stochastic algorithms for discrete parameter simulation optimization. *IEEE Transactions on Automation Science and Engineering*, 8(4):780–793, 2011b.
- S. Bhatnagar, H.L. Prasad, and L.A. Prashanth. *Stochastic Recursive Algorithms for Optimization*, volume 434. Springer, 2013.
- Shalabh Bhatnagar and Vivek S Borkar. Multiscale chaotic SPSA and smoothed functional algorithms for simulation optimization. *Simulation*, 79(10):568–580, 2003.
- S. Bhulai, G. Koole, and A. Pot. Simple methods for shift scheduling in multi-skill call centers. *Manufacturing and Service Operations Management*, 10(3), 2008.
- VS Borkar. An actor-critic algorithm for constrained Markov decision processes. *Systems & control letters*, 54(3):207–213, 2005.
- V.S. Borkar. *Stochastic approximation: a dynamical systems viewpoint*. Cambridge Univ Pr, 2008.
- C. Brickner, D. Indrawan, D. Williams, and S.R. Chakravarthy. Simulation of a stochastic model for a service system. In *Winter Simulation Conference*, pages 1636–1647, dec. 2010. doi: 10.1109/WSC.2010.5678905.
- M.T. Cezik and P. L’Ecuyer. Staffing multiskill call centers via linear programming and simulation. *Management Science*, 54(2):310–323, 2008.
- H.F. Chen, T.E. Duncan, and B. Pasik-Duncan. A kiefer-wolfowitz algorithm with randomized differences. *IEEE Transactions on Automatic Control*, 44(3):442–453, 1999.
- P.E. Gill, W. Murray, and M.H. Wright. *Practical optimization*. Academic press, 1981.
- M.W. Hirsch. Convergent activation dynamics in continuous time networks. *Neural Networks*, 2(5):331–349, 1989.
- Harold J. Kushner and Dean S. Clark. *Stochastic approximation methods for constrained and unconstrained systems*. Springer-Verlag, 1978. ISBN 0-387-90341-0.
- Harold Joseph Kushner and George Yin. *Stochastic approximation and recursive algorithms and applications*. Springer, 1997. ISBN 0-387-00894-2.
- J. P. Lasalle and S. Le fschetz. *Stability by Liapunov’s Direct Method with Applications*. Academic Press, New York., 1961.
- P. Marbach and J.N. Tsitsiklis. Simulation-based optimization of Markov reward processes. *IEEE Transactions on Automatic Control*, 46(2):191–209, 2001.

- A. Mas-Colell, M.D. Whinston, and J.R. Green. *Microeconomic theory*. Oxford University Press, 1995. ISBN 9780195073409.
- H.L. Prasad, L.A. Prashanth, N. Desai, and S. Bhatnagar. Adaptive smoothed functional algorithms for optimal staffing levels in service systems. *Service Science*, 5(1):29–55, 2013.
- L.A. Prashanth, H.L. Prasad, N. Desai, S. Bhatnagar, and G. Dasgupta. Stochastic optimization for adaptive labor staffing in service systems. *Service-Oriented Computing*, pages 487–494, 2011.
- T.R. Robbins and T.P. Harrison. A simulation based scheduling model for call centers with uncertain arrival rates. In *Winter Simulation Conference*, pages 2884–2890, 2008.
- J.C. Spall. Multivariate stochastic approximation using a simultaneous perturbation gradient approximation. *IEEE Transactions on Automatic Control*, 37(3):332–341, 1992. ISSN 0018-9286.
- J.C. Spall. A one-measurement form of simultaneous perturbation stochastic approximation. *Automatica*, 33(1):109–112, 1997. ISSN 0005-1098.
- J.C. Spall. Adaptive stochastic approximation by the simultaneous perturbation method. *IEEE Transactions on Automatic Control*, 45(10):1839–1853, 2000.
- J. Spohrer, P.P. Maglio, J. Bailey, and D. Gruhl. Steps toward a science of service systems. *Computer*, 40(1):71–77, 2007.
- A. Verma, N.V. Desai, A. Bhamidipaty, A.N. Jain, J. Nallacherry, S. Roy, and S. Barnes. Automated optimal dispatching of service requests. *SRII Global Conference*, 2011.
- S. Wasserkrug, S. Taub, S. Zeltyn, D. Gilat, V. Lipets, Z. Feldman, and A. Mandelbaum. Creating operational shift schedules for third-level IT support: challenges, models and case study. *International Journal of Services Operations and Informatics*, 3(3):242–257, 2008.